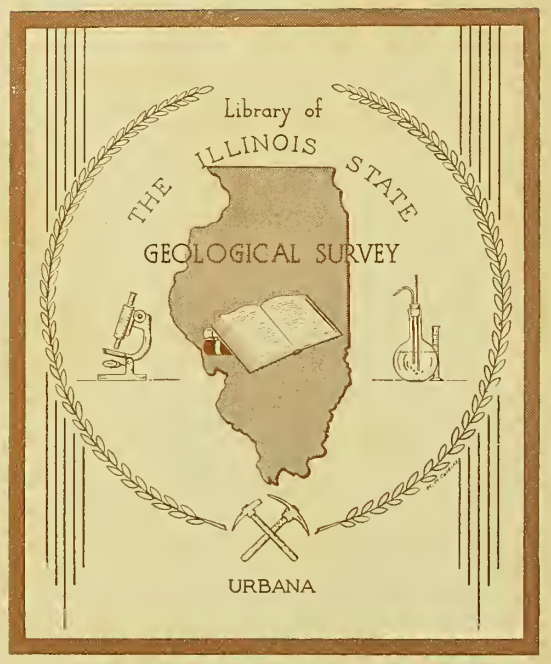

ENVIRONMENTAL GEOLOGY NOTES

AUGUST 1972 · NUMBER 55

USE OF CARBONATE ROCKS FOR CONTROL OF SULFUR DIOXIDE IN FLUE GASES

Part I. Petrographic characteristics and physical properties of marls, shells, and their calcines

R. D. Harvey, R. R. Frost, and Josephus Thomas, Jr.

ILLINOIS STATE GEOLOGICAL SURVEY

JOHN C. FRYE, Chief · Urbana 61801

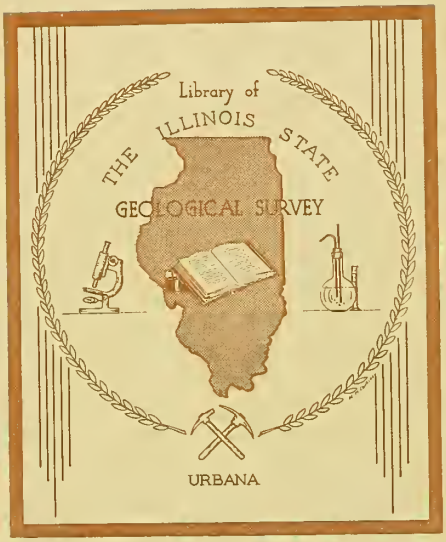
Library of
THE ILLINOIS STATE
GEOLOGICAL SURVEY
URBANA

USE OF CARBONATE ROCKS FOR CONTROL OF SULFUR DIOXIDE IN FLUE GASES

PART I. PETROGRAPHIC CHARACTERISTICS AND PHYSICAL PROPERTIES OF MARLS, SHELLS, AND THEIR CALCINES

CONTENTS

TABLES

APPENDIXES

ILLUSTRATIONS

Figure Page

Plate

USE OF CARBONATE ROCKS FOR CONTROL OF SULFUR DIOXIDE IN FLUE GASES

PART I. PETROGRAPHIC CHARACTERISTICS AND PHYSICAL PROPERTIES OF MARLS, SHELLS, AND THEIR CALCINES*

R. D. Harvey, R. R. Frost, and Josephus Thomas, Jr.

ABSTRACT

Thirty-seven operating pits and some discontinued pits in fresh-water lake marls and bog marls in the northeastern quarter of the United States were sampled, and the mineralogical, textural, and pore-volume properties of the samples were determined. The pore volume and surface area of the calcination product of each sample were also determined. In addition, selected samples of coquina and shells, obtained from deposits along the Gulf Coast, were similarly studied. The properties measured are thought to be indicative of the capacity of carbonate rocks to absorb SO_2 from flue gases in dry and wet scrubbing processes.

Annual production of marl, according to the U.S. Bureau of Mines, has been less than 3 million tons for several years, although the tonnages could be vastly increased upon demand. At present, nearly all lakes and bog marls produced are used as agricultural limestone and soil conditioners, principally in northern Indiana and southern Michigan.

The $CaCO_3$ content of most marls sampled was between 80 and 90 percent. The principal impurities are quartz silt and organic matter. The pore volume ranges mainly between 0.3 and 0.6 cc/g. The size of the pores in marls is mainly between 0.1 μ and 10 μ in diameter. Upon calcination (at 850° C to 950° C, for 5 to 10 minutes, under high nitrogen gas flow rate), virtually all the newly formed pores are less than 0.1 μ in diameter and the surface area of the calcines is high, mainly in the range of 20 to 30 m^2/g calcine. These properties indicate good potential for utilization of marls in SO_2 control processes. The smaller pore volumes of shells and coquinas and the lower surface areas of their calcines suggest that these materials have lower SO_2 capacity and reactivity than the marls.

* Part of the work upon which this publication is based was performed pursuant to Contract No. 68-02-0212 with the U.S. Environmental Protection Agency.

INTRODUCTION

Air pollution caused by emission of sulfur oxides from power plants is a major environmental problem, especially in highly industrialized areas. Current research on this problem includes the use of limestone and related materials to react with sulfur dioxide (SO_2) and prevent its emission. Several processes based on this chemical reaction have been proposed and are being tested at a number of plants. If one of these processes can be proved technically feasible and reliable, it will be of considerable importance, because these processes generally require the lowest capital and operating costs of any prospective process for SO_2 control. Of the various processes being considered by power companies and others, the wet lime-limestone scrubbing process is favored as the short-range solution for removal of SO_2 from stack gases (Dibbs, 1971).

Tests of Borgwardt (1970), Attig and Sedor (1970), and Coutant et al. (1971) of a sample of calcareous marl from Michigan and subsequent tests of two other samples of similar marl (Harvey and Steinmetz, 1971) have shown that these incoherent (soft) types of carbonate rocks have a relatively high capacity for reaction with SO_2 at elevated temperatures such as those that occur in coal-fired boilers. Other relatively incoherent types, illustrated by two samples of chalk and a sample of oolitic aragonite sand, also showed high SO_2 absorption capacities (Harvey and Steinmetz, 1971). It is thought that these types of carbonates, upon heating, yield calcines having large pore volumes and high surface areas. These properties of the calcines are considered the major factors affecting the relative SO_2 sorption capacities of samples of carbonate rocks. In addition, a marl and a chalk showed high reactivity with SO_2 in a laboratory wet scrubbing system (Drehmel, 1971). Since so few samples have been tested, detailed examination and testing of a number of these highly reactive rock types are needed for efficient selection of carbonate materials for maximum desulfurization by limestone processes.

The purposes of this study are to locate and sample a number of deposits of marls, chalks, and sea shells; to characterize the samples petrographically and chemically; to determine the grain-size and pore-volume distribution of the samples; and to relate these properties to the pore-volume distribution and the surface area of the calcined products.

Samples of sea shells are included in this study because of their similarities to the oolitic aragonite sand, which was determined to have high absorption capacity in previous tests. Both the oolitic sand and the sea shells originate in nearshore marine environments; both consist of very fine-grained fibrous carbonate crystallites; and many sea shells consist of aragonite.

This interim report covers the first 12 months' work on the project. During this time attention was focused on the study of fresh-water (lake and bog) marls and sea shells. The remaining period of this project (to March 1973) will be devoted to studies of chalks.

Definitions of Sample Types

It will be useful to clarify and define the types of carbonate materials studied. Marl is not a precise petrologic term, and geologists from various parts of the world use this term to describe a variety of rocks. The term marl as used in this report is restricted to a soft, incoherent, and very fine-grained material that is composed largely of calcite and is found in some fresh-water lakes and bogs. A lake marl is a marl that occurs beneath a considerable body of water (more than about 25 acres), and a bog marl is one that occurs beneath a bog—a tract of wet land covered with dense vegetation and, in many cases, with peat. In this report, the classification of a sample of marl as a lake or bog marl is based on the presence or absence of a natural lake at the sample locality. If such a lake does not occur in the specific locality of a sample, the sample is classified as a bog marl. It is recognized that most bogs evolved from a lake by overgrowth of vegetation. However, this classification of the samples was made primarily in the field at the time of sample collection and was considered potentially useful. Some marls have a pronounced sandy texture or "feel" due to the presence of abundant particles mainly 100 μ to 2000 μ (microns) in size. These marls are referred to as tufaceous marls. Some calcareous shales, calcareous siltstones, and very clayey or silty limestones, frequently phosphatic and occurring in the southeastern part of the United States, are described in older geologic literature as marls. These rocks, marine in origin, are unlike the lake marls in composition and texture and are not classified as marls in this study.

Coquina is a type of carbonate rock that is composed dominantly (> 75 percent) of shells and shell fragments or calcareous tests of invertebrates that are partly lithified, or cemented, into a rock material. Geologic literature contains references to shell marls and marls that formed under marine environments and contain abundant shells and shell fragments with various amounts of sand, silt, and clay. These do not resemble the fresh-water marls in texture. For clarity, the so-called shell marls, when they contain abundant calcareous shells, are classified in this report as coquinas.

Shell is a type of carbonate material that consists of shells of a variety of invertebrates that accumulate in large quantities in certain localities under shallow water. A single shell is hard and consists of calcite or aragonite crystallites. The shells are not cemented together, and they are dredged for commercial purposes from nearshore deposits, mainly along the Gulf Coast in this country.

Chalk, as used in this report, is a very fine-grained, porous, and partly incoherent carbonate rock composed of 75 percent or more $CaCO_3$ and containing abundant minute marine fossils. Geologic literature contains references to chalks that are actually calcareous siltstones or very impure chalks that contain as little as 30 percent $CaCO_3$. These rocks should not be considered chalks and are excluded from this study.

Uses and Production of Marl

During the early 1900's, considerable use was made of marl as a source of CaO for the manufacture of natural and portland cement. Plants were

located principally in New York, Pennsylvania, Ohio, and Indiana. Production of marl for use in cement decreased in the 1930's, and by 1940 little or no marl was used for this purpose.* However, marl has long been used as a source of agricultural limestone, and marl, as defined here, continues to be produced almost entirely for this purpose. In 1968, 1,211,015 tons of calcareous marl* was produced in the United States (U.S. Bureau of Mines, 1969). In 1969 production increased to 2,490,000 tons (U.S. Bureau of Mines, 1971). Indiana and Michigan are the major marl-producing states. In 1971 there were 22 producers of marl at 24 pits in Michigan (Segall, 1972), and 29 pits were active in Indiana (Purdue University, 1971). During the summer of 1971, there were two active marl pits in Minnesota and one active pit in each of the states of Virginia, New York, and Wisconsin. Frequent discussions with owners of marl deposits suggest that if a new market or new use for marl were developed, production could be vastly increased.

With few exceptions, marl is mined by dredging a channel through it with a crane and stockpiling it along the bank to drain the water (fig. 1). After drying for a month or so, the material in the stockpile is turned over frequently to promote further drying. However, the marl in one pit examined was dry enough that it could be disked and loaded onto trucks for delivery; another pit was pumped sufficiently dry to enable direct loading onto trucks.

Sample Localities and Sample Processing

Geologic literature was surveyed to find localities of marls in the contiguous states of the United States. With rare exception, all known lake and bog marls occur in the northeastern part of the country. These marls are associated with the fresh-water glacial lakes and bogs that formed during the Pleistocene Epoch of geologic time.† An annotated bibliography of the occurrences and geology of marls in the northeastern part of the country is given in appendix 1. Thirty-seven deposits were selected for field examination and sampling. In addition, two samples of coquina, three samples of shells—one calcitic, one aragonitic, and one a mixture of the two—were obtained for study. A sample of a sludge—a calcite-rich and fine-grained waste product from a paper manufacturing plant— was also obtained. A total of 68 samples was collected from the deposits (fig. 2). Specific localities of the deposits and remarks on the deposits and samples are given in appendix 2. In some cases, samples were taken from stockpiles by digging a shallow hole at several different places on the stockpile and taking about half a liter of marl from the bottom of each hole. About 10 to 20 pounds of marl was taken for each sample. Many samples were taken by hand-augering the uppermost beds. The relative position of these samples within the strata of the deposit and the thickness of the marl represented are given in appendix 2.

A comprehensive series of laboratory tests and analyses were made on the samples so that relations between the pore volume and surface area of

---

* Coquina continues to be used in the manufacture of portland cement in Virginia and elsewhere and is included in U.S. Bureau of Mines production tables under calcareous marls.

† The Pleistocene Epoch covers the time interval popularly known as the "Ice Age," which began approximately 1 million years ago and includes the Holocene (Recent) Stage. Marl appears to be forming in some lakes today.

Fig. 1 - Marl production pit.

the marls and those of their calcines could be ascertained. To provide small samples for the tests, the larger field samples were dried, the clods broken, and the samples thoroughly mixed and quartered. Each sample was quartered until approximately 400 grams of it was obtained. One quarter of this material was sieved to obtain the 16x18, 18x40, 40x50, 50x170, and the 170x200 mesh fractions. The 16x18, 40x50, and 170x200 mesh fractions were separated for pore-volume and calcination tests. Another quarter was further reduced to pass a 100 mesh screen. This sample was subjected to particle-size, mineralogical, and chemical analyses. Thin sections (< 10 μ thick) were prepared from the 18x40 and 50x170 fractions for petrographic and crystallite grain-size analyses with a Quantimet image analyzing computer. The particles larger than 16 mesh were examined with the scanning electron microscope (SEM) equipped with an X-ray analyzer. Lastly, half of the 400 gram sample was subjected to Harvard miniature compaction tests (Wilson, 1970).

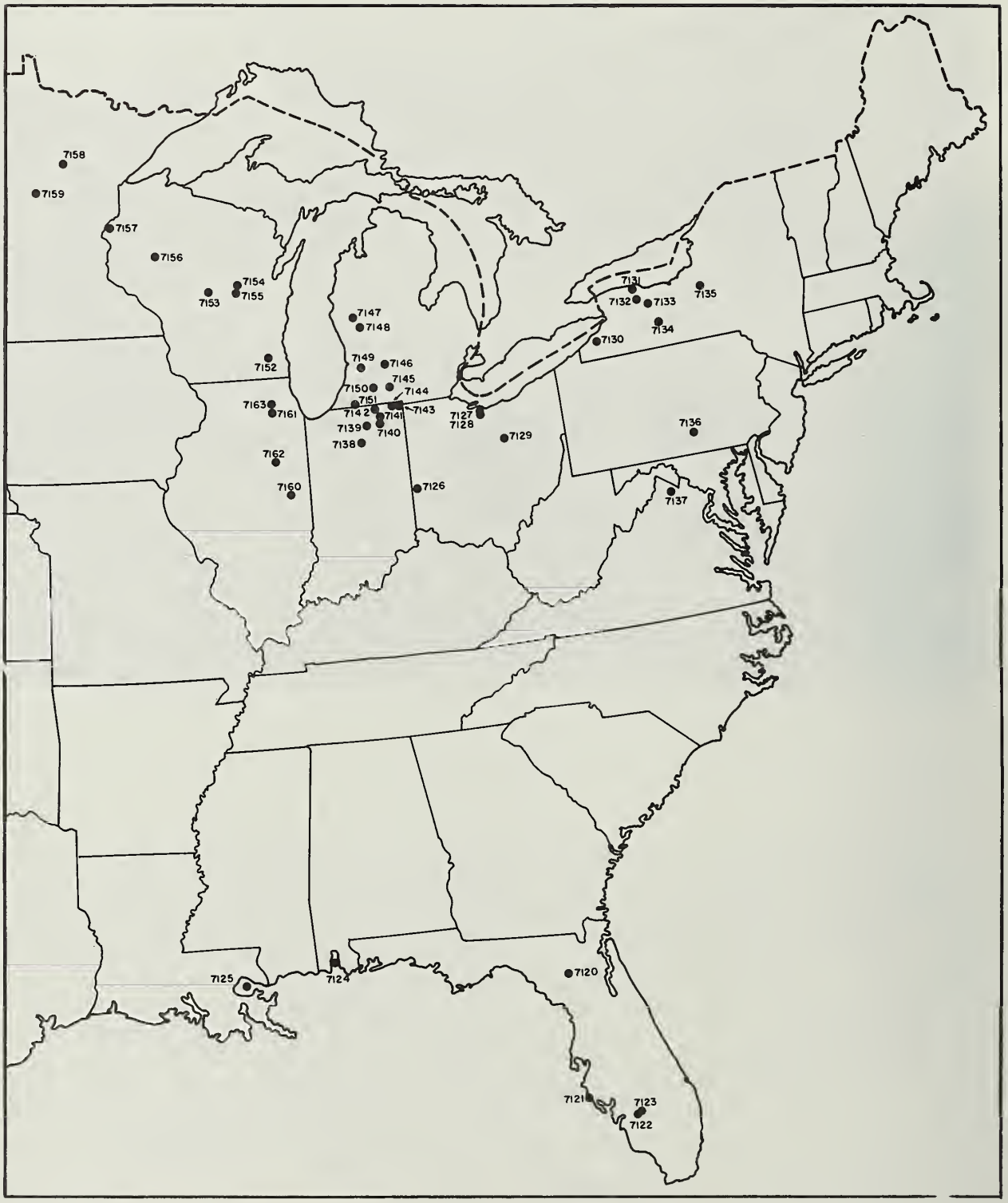

Fig. 2 - Sample localities.

CHARACTERIZATION OF SAMPLES

Petrographic Description of Sample Types

Shells and Coquina

Samples classified by type as shells are numbers 7121, 7124, and 7125 (app. 2); these were collected from deposits along the Gulf of Mexico—7121 in Florida, 7124 in Alabama, and 7125 in Louisiana (fig. 2). More than 70 percent (by weight) of the shells in 7121A are bivalves of Chione cancellata (family Veneridae). A few bivalve shells belonging to other families also occur. Less than two percent of the sample consists of gastropod shells. The shells in this sample consist mainly of the mineral aragonite. Sample 7121B, augered from below 7121A, has types of shells identical to those in 7121A but differs in that a considerable amount of quartz sand is present. These samples were obtained from an offshore bar, and similar shells occur all along this bar. According to H. S. Puri (1971, personal communication), the sample is from the Anastasia Formation (Pleistocene in age), which is a source of commercial shells elsewhere in Florida.

Each of the other two shell samples consists of only one type of shell. Sample 7124 contains shells of clams (Rangia), 3/4 inch to 1 1/4 inches across, gray, and consisting of aragonite. Sample 7125 contains gray shells of oysters (Ostrea) about 4 inches long and 2 inches wide and composed of calcite. Both of these samples are from shell beds that are commercially dredged and processed.

Microscopic examination reveals that the shells consist of fibrous crystallites of aragonite or calcite (pl. 1). In the clam shells, the fibers are laminated in two or more directions (pl. 1A) and the fibers in each lamella are nearly parallel to each other. In Chione, pores 0.1 μ to 0.5 μ across occur intermittently along the boundaries of the fibers (pl. 1B), and in the oyster shells, larger pore channels occur (pl. 1C). Shells observed in transmitted polarized light are birefringent and each fiber has a slightly different orientation from that of neighboring fibers.

Coquinas were obtained from two deposits, 7120 and 7122 (app. 2). These samples consist of shells and other fossils composed of calcite; however, 7122B contains a few aragonitic shells.

Sample 7120 is a porous coquina, soft, white, and chalky, with poorly defined bedding. Locally the coquina is stained brown by traces of iron; otherwise, the material is uniform and pure. Certain beds consist entirely of lithified shells and orbitoid foraminifera tests. The latter are about the size and shape of a penny. In other beds, in which the shells are not so abundant, the

A. Clam shell from 7124 ⌊ 20μ ⌋ (x930)

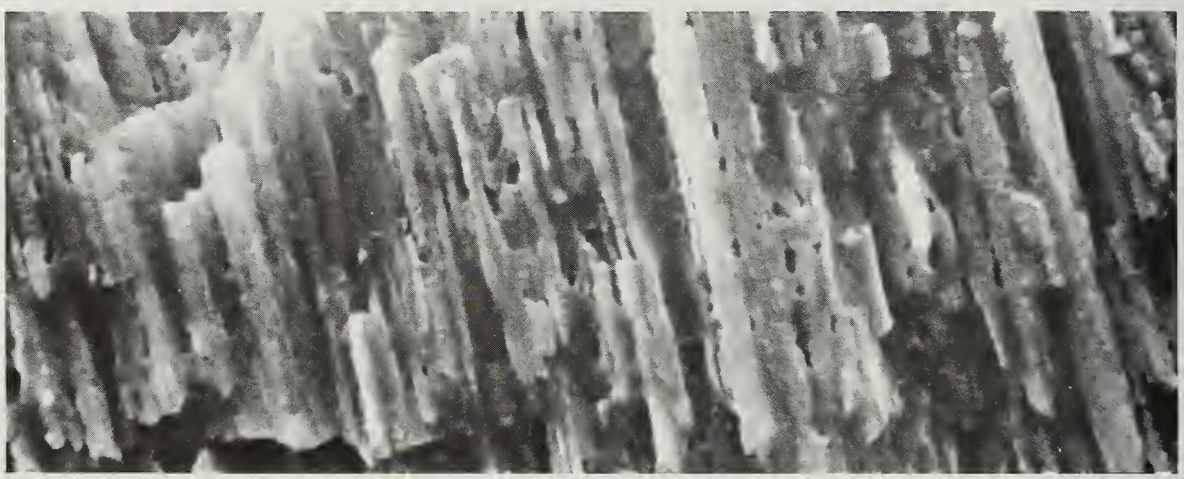

B. Chione from 7121A ⌊ 5μ ⌋ (x4120)

C. Oyster shell from 7125 ⌊ 20μ ⌋ (x1100)

Plate 1 - Characteristic textural features of shells.

stone is porous and contains very fine-grained (1 μ to 4 μ across) calcite. The sample was taken from beds of the Crystal River Formation, Ocala Group (Eocene in age). Several operating quarries produce crushed stone from this geologic unit.

Samples 7122A and B and 7123 are from the Caloosahatchee Marl (Pleistocene in age). Samples 7122A and B are coquinas containing abundant gastropods up to 4 inches long, numerous bivalves, irregular and cylindrical "worm tubes," and other calcareous fossils and fossil fragments. Fine-grained calcite and quartz silt occur between the shells. Sample 7122A overlies 7122B and is harder and of higher purity. The beds sampled grade laterally into more impure coquinas and into quartz-rich sands containing only a few shells less than 3 miles to the northeast (sample 7123).

Microscopic examination shows that the coquina samples consist of fibrous and laminated calcium carbonate of the type illustrated in plate 1. The foraminifera tests in 7120 consist of equant grains (1 μ to 2 μ across) with considerable pore space around most of the grains. The grain sizes in shells and coquinas average approximately 6 μ.

Lake Marls and Bog Marls

The distinction between lake marls and bog marls is based on the presence or absence of a natural lake immediately above the collection site. The samples designated as lake marls (app. 2) do not differ greatly from bog marls. Both types consist overwhelmingly of very fine-grained gray to light buff calcite. They are very soft and incoherent mud-like materials and frequently contain organic remains of plants. Conspicuously scattered through marls are mollusk shells (pl. 2), specimens and varieties of gastropods being more abundant than those of bivalves. Both pulmonate (with lungs) and branchiate (with gills) gastropods occur. The mollusk shells are very easily broken, and in all specimens examined they consist of the aragonite form of $CaCO_3$. Gastropod specimens are frequently 1/2 to 1 cm across, whereas the other types of shells present are usually 1 to 2 mm or less across. The larger shells are conspicuous in the marl because their color is milky white while the surrounding fine-grained calcite is darker in color. The darker color is due principally to the occurrence of organic matter and moisture. Marls containing little or no organic matter are nearly white when dry.

The major inorganic impurities in marls are quartz, as partly rounded grains 4 μ to 30 μ in diameter, and a few similarly sized and shaped grains of feldspar. These impurities are present in nearly every sample of marl and are scattered throughout the marl material rather than being concentrated in certain layers. The abundance of these grains is proportional to the amount of SiO_2 and Al_2O_3 observed in the samples, as discussed later.

Study of lake marls by electron microscopy (pl. 3, A-F) shows the character of the grains and the high porosity of the samples. The micrographs shown illustrate characteristic textural features of the lake marls studied. Crystallite grain size, measured from more than five micrographs of each sample of the 14 lake marls, ranges from 0.1 μ to over 16 μ; most grains have a diameter between 0.5 μ and 2 μ. In large part, these marls consist of agglomerate particles composed of several grains or crystallites (0.5 μ to 2 μ) weakly

A. Pulmonate gastropod, Gyraulus altissimus (Baker)

B. Branchiate gastropod, Amnicola leightoni (Baker)

C. Bivalve, Pisidium sp.

D. Pulmonate gastropod, Physa sp.

Plate 2 - Common mollusks from Pleistocene marls (x10).

A. Sample 7138 5μ (x2540)

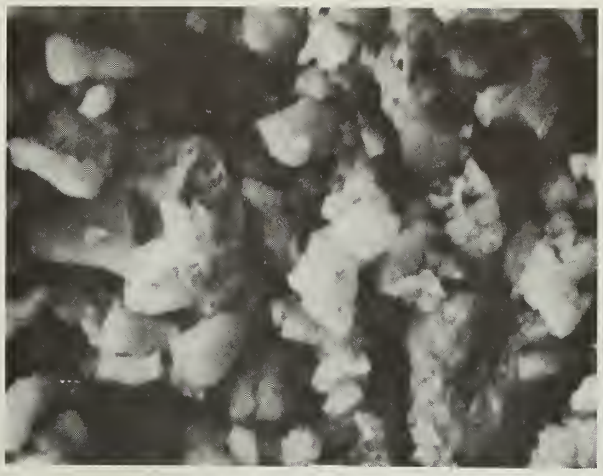

B. Sample 7142 5μ (x2510)

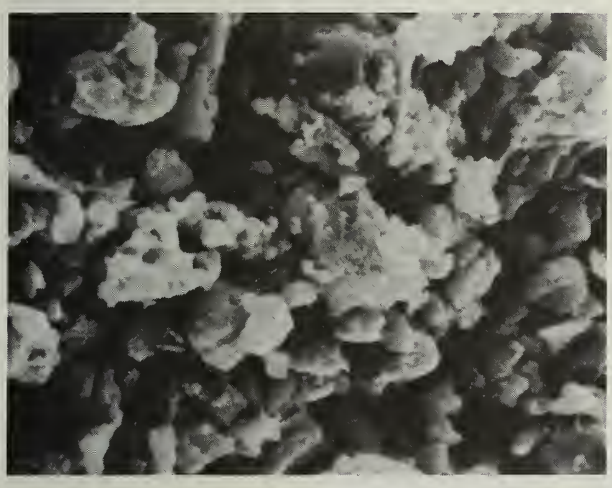

C. Sample 7142 5μ (x2240)

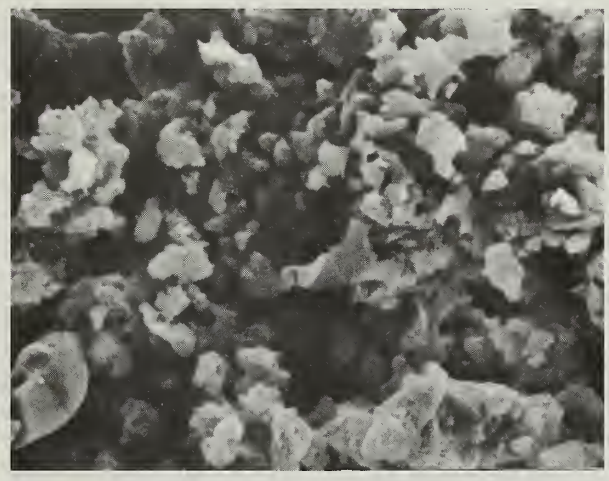

D. Sample 7134A 5μ (x1970)

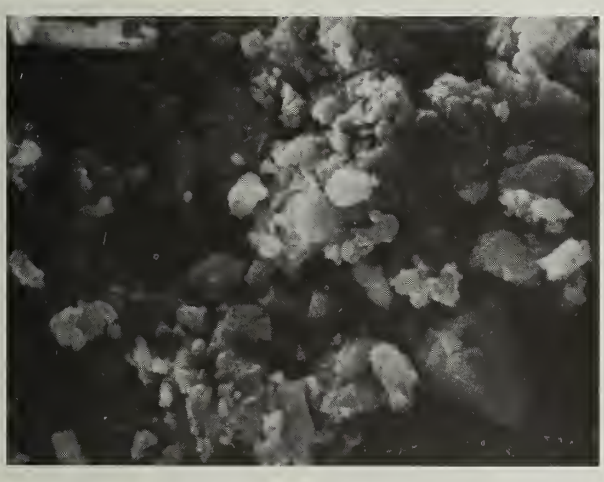

E. Sample 7158 5μ (x2670)

F. Sample 7157C 5μ (x2210)

Plate 3 - Characteristic textural features of lake marls.

A. Sample 7128A 5μ (x3020)

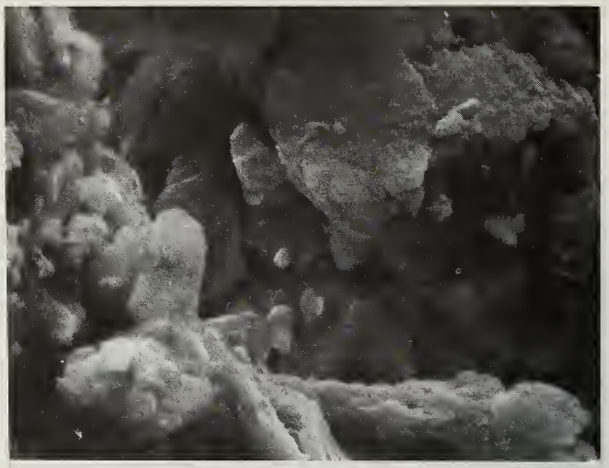

B. Sample 7133 5μ (x2580)

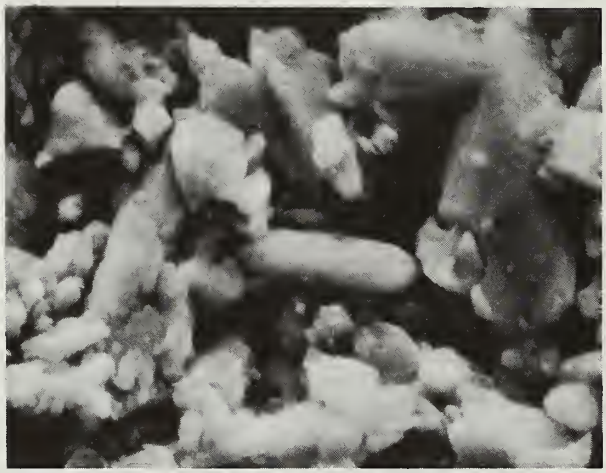

C. Sample 7133 5μ (x2150)

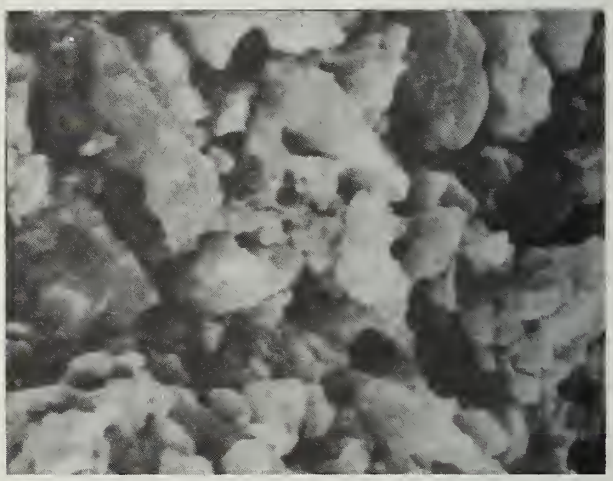

D. Sample 7151B 5μ (x3250)

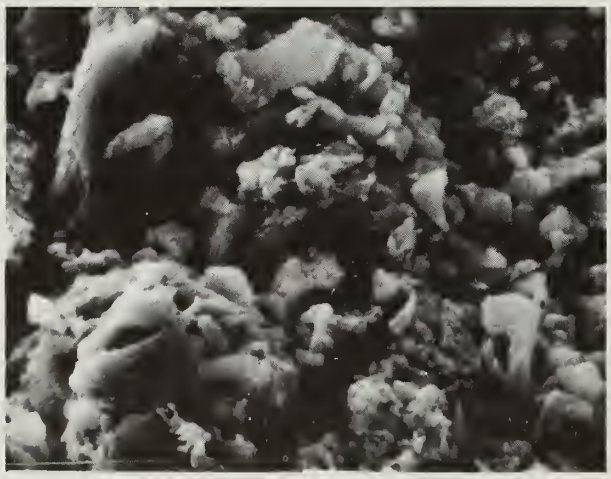

E. Sample 7162B 5μ (x1890)

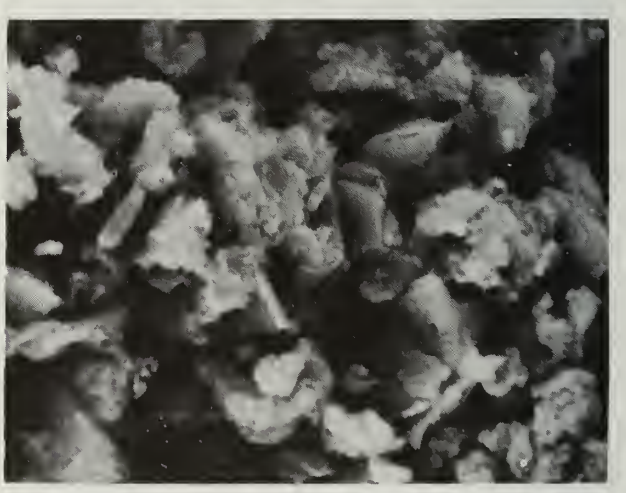

F. Sample 7163B 5μ (x2350)

Plate 4 - Characteristic textural features of bog marls.

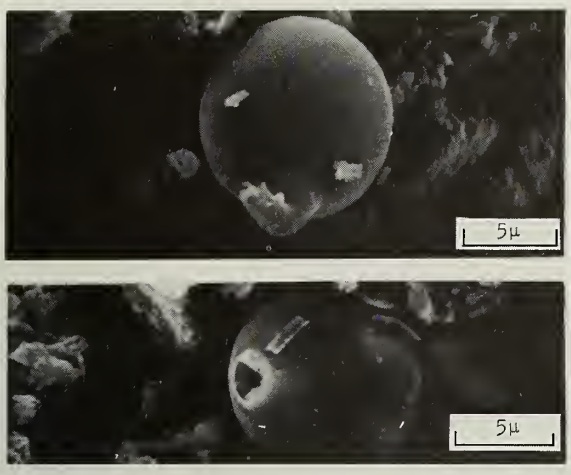

A. Spores in 7162C (x2500)

B. Framboidal pyrite (x2430)

C. Tubules in tufaceous marls (x20)

D. Diatom Cymbella sp. (x1990)

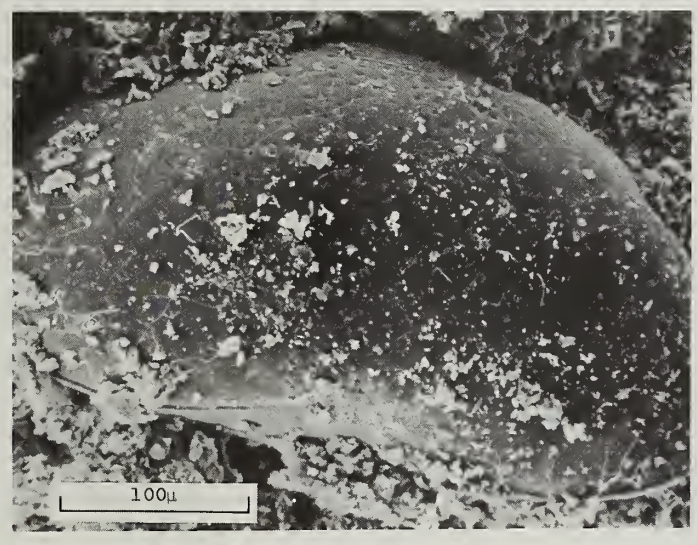

E. Ostracod valve (x244)

Plate 5 - Selected types of particles that occur in marls.

held together to form porous particles (especially noted in pl. 3F). In some areas, grains and particles are not clearly distinguished, such as in the right hand part of the large particle in the lower left of plate 3A. In this case, it is interpreted that the nodes present there are grains. Similarly, the nodes on the particle in the center of plate 3C are interpreted to be grains.

Most bog marls consist mainly of very fine-grained calcite (pl. 4, D, E, and F) and resemble lake marls in many respects. Bog marls tend to be somewhat coarser grained than lake marls.

A tubular particle is found in 75 percent of the marls and is usually most abundant in bog marls. These particles are about 1/4 to 1 mm in diameter and 1 to 10 mm long (pl. 5C). The interior of these particles contains several open channels that run parallel to the long axis. Inspection of the outer surface of the tubules (pl. 4, A, B, and C) shows randomly oriented, and interlocking grains of calcite that are larger than most of the other calcite grains in the marl. These tubules are the most coherent particles in marls although they readily break apart when a few are rolled together between one's fingers. When these tubules are very abundant, the marl is designated as tufaceous (app. 2).*

Quartz and a few feldspar grains occur in bog marls as in previously described lake marls. Unusual and rare particles, found in a few samples of marls, are spores (pl. 5A); framboidal pyrite (pl. 5B)—spheroids 10 μ to 30 μ in diameter that consist of crystals (mainly 1 μ octahedrons in this case) of pyrite (FeS_2); diatoms (pl. 5D)—delicate, siliceous skeletons of aquatic algae, especially abundant in 7162A; and ostracod carapaces (pl. 5E)—shells of minute bivalve crustacean fossils.

Particle Size and Grain Size of Samples

The samples were tested in three ways for their particle size and grain size. The term grain refers to a single crystalline unit or crystallite. The term particle refers to a granular unit that may be a single grain but most frequently consists of several grains. The sedimentation method of size analysis yields particle-size data in most materials, including marls. Microscopic observations with polarized light allows measurement of the size of individual grains.

In each of the marl samples, microscopic measurements were made of the grains in two sieve-size fractions. Several hundred particles of both fractions were embedded in epoxy, and thin sections approximately 5 μ to 10 μ thick were prepared. Fifty or more different fields of view in these sections were analyzed with the Quantimet under cross-polarized light with an X40 objective lens. Resolution was approximately 0.5 μ. Thus, many grains of less than 1 μ in the thin sections were not detected by the Quantimet. However, the thin

* Davis (1901), Thiel (1930), and others have made detailed studies of such tubular structures and concluded that they were formed by the precipitation of $CaCO_3$ on the stems of Chara plants and, in places, several crystallites were sufficiently interlocked to form a coherent sediment particle, which was deposited on the bottom of the bog after the death of the plant.

sections give representative and relative measures of the grain size of the samples. Grain size as measured by the Quantimet for each field of view is expressed in terms of the mean chord length in microns. The mean chord length ($\bar{C}$) was computed from the Quantimet output readings of grain area (A) and the grain area projection (P), according to:

$$\bar{C} = \frac{AL}{PM}$$

where L is the length of the magnified image (field of view) and M is the magnification.

The mean chord length is related to the maximum diameter (D) of spheres according to:

$$D = 1.274\ \bar{C}.$$

Another parameter of the grain texture obtained from Quantimet analysis is a measure of the total length of the boundaries of the grains. Since the circumference (or boundary) of a circle is π D, the grain boundary length per unit area (B) expressed in mm/mm^2 can be computed from P for each field of view according to:

$$B = \pi \frac{M}{L} P.$$

For two specimens with the same size grains, differences in observed B reflect differences in the mean shape and roundness of the grains in the specimens. Averages of the 50 or more values of $\bar{C}$ and of B determined for each sample were computed and taken to be characteristic of the sample (table 1). In addition to the petrographic thin-sections, many of the scanning electron micrographs taken for this study were of sufficient quality and contrast to enable their analyses by the Quantimet procedures (table 1).

The results of the Quantimet analyses show the mean chord length of the bog marls to range from 1.8 μ to 5.7 μ. The average is 3.4 μ. The range of $\bar{C}$ for lake marls is 2.1 μ to 4.4 μ, with an average (2.8 μ) slightly smaller than the average for bog marls. In many samples, though not all, the mean chord length measured on the electron micrographs is smaller than that from the thin sections of the same samples. Two disadvantages are inherent in analysis of the electron micrographs: (1) to obtain a representative sample of grains, one must take a very large number of micrographs, and (2) the contrast of the grains is not sufficient in many micrographs to obtain accurate results with the Quantimet.

Selected samples of the purer marls were subjected to particle-size analyses by the sedimentation method. Clods of air-dried marl were broken up to pass 100 mesh (0.15 mm).* This sample was then mixed with distilled water

* A very small portion of the marl samples, mainly Chara tubules, required only slight grinding to pass 100 mesh. All that was done to the sample was to break up the air-dried clumps or particles of marl.

TABLE 1 — TEXTURAL ANALYSES OF SAMPLES

Sample number	Quantimet results: Mean grain chord length (μ) — Thin sections*	Quantimet results: Mean grain chord length (μ) — Electron micrographs	Quantimet results: Total grain boundary length (mm/mm^2) — Thin sections	Quantimet results: Total grain boundary length (mm/mm^2) — Electron micrographs	Mean particle size† (μ)
7120	4.1		2470		
7122A	7.5				
7122B	6.2		3483		
7125	5.4		3040		
7126A	3.8		2945		40.0
7127A	6.6		2964		
7127D	2.6		2185		
7128A	4.2		2622		
7128B	5.7	1.54	2394	680	42.0
7129	3.5		2698		
7130	3.3		2926		
7131A	3.2		3059		
7131B	2.7		2090		
7131C	4.0		3002		
7132A	3.8		4180		
7132B	4.3	2.05	1881	611	
7132C	2.7	2.22	2964	1264	
7132D	3.1	1.84	2964	950	8.2
7133	4.1	4.24	2375	482	22.0
7134A	2.2	1.71	2983	876	
7136	3.0		2052		
7137	3.0		3610	1083	6.7
7138	2.4	3.74	3211	447	35.4
7139	2.7	3.11	2185	667	
7140	3.2		2679		30.0
7141	2.7	2.85	2489	755	10.5
7142	2.1	1.81	2888	965	24.2
7143A	2.6	1.41	2812	1300	22.3
7144A	2.6		2527	918	
7145A	2.1	1.53	2755	966	
7146A	3.0		3192		
7147A	2.8	2.17	2926	740	
7148	3.4	1.62	3078	1103	
7149A	2.8	2.21	2432	842	39.0
7149B		2.37		849	22.1
7150	4.4	0.41	2869	1161	7.6
7151A	3.3	4.05	1254	389	
7151B	2.9	1.48	2774	1008	
7151C	2.7	2.00	4237	848	
7152	1.8		4294		29.5
7154	3.9		2546		
7155	3.0		2831		
7157A	3.2	2.85	3686	794	9.9
7157B	3.1		1900		
7157D	2.5		1672		
7158	2.4	1.30	1824	1308	
7159	2.5	2.66	1938	742	
7160	3.4		2546		
7161	3.5				
7162A	4.7	3.90	1634	497	
7162B	4.0	2.01	1463	453	
7162C	4.0	1.54	2831	783	
7162D	3.9	1.72	1330	617	
7163A		1.72		702	
7163C	4.0		1976		8.6

*Excludes grains less than 1μ in diameter, the limit of optical resolution of the microscope.

†The size corresponding to the 50% point on the cumulative curves (figs. 3-6); determined by sedimentation methods on samples dispersed and vigorously stirred in water for 15 minutes.

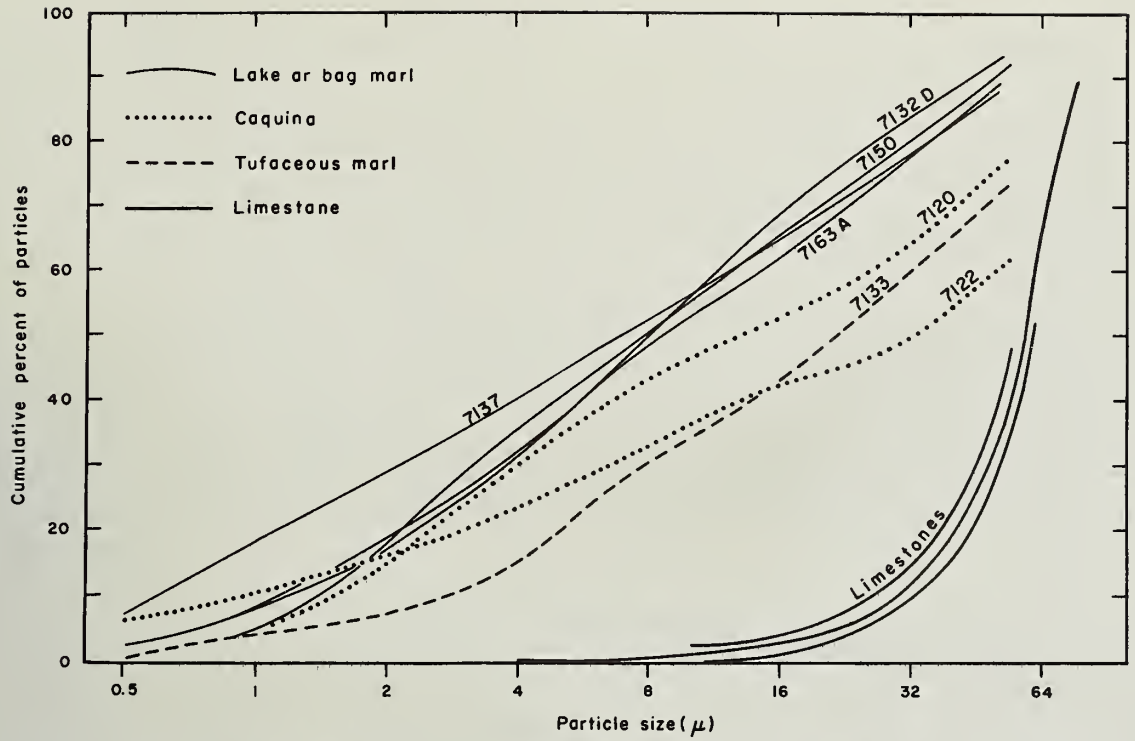

Fig. 3 - Particle-size distribution of selected marls and coquinas. For comparison, results are shown for three coherent and hard limestones (Types 2, 3, and 4, Harvey and Steinmetz, 1971) that were crushed and pulverized for 2.5 hours in a laboratory ball mill.

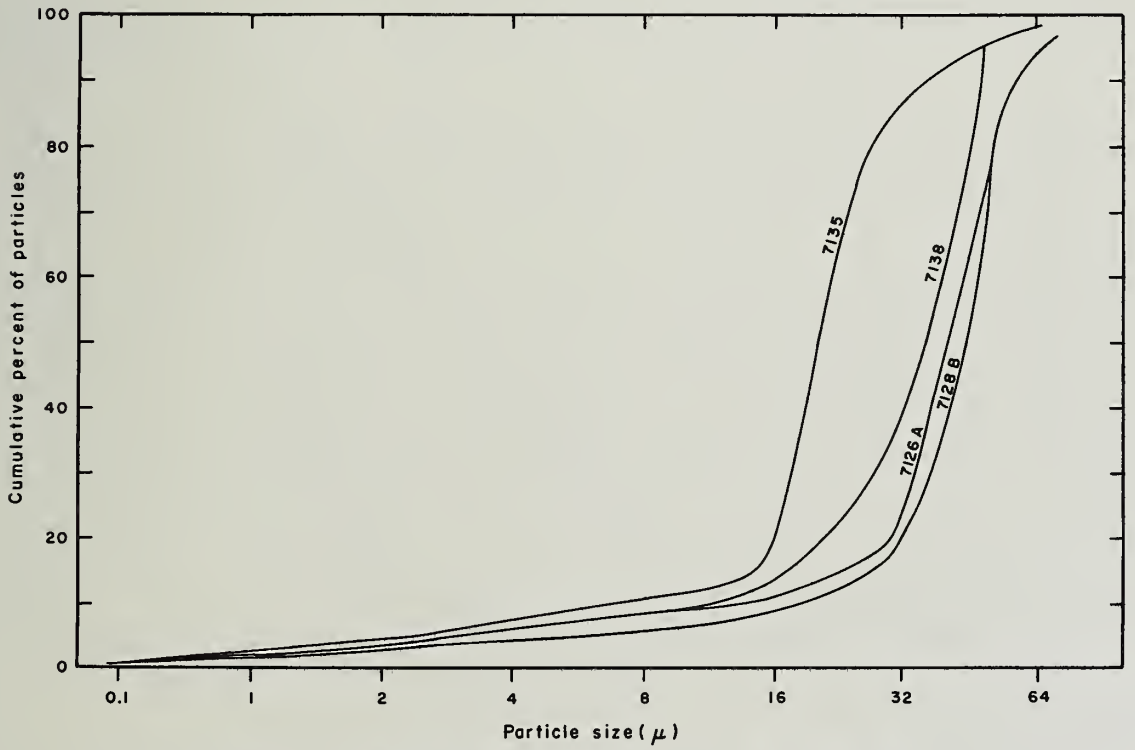

Fig. 4 - Particle-size distribution of marl samples.

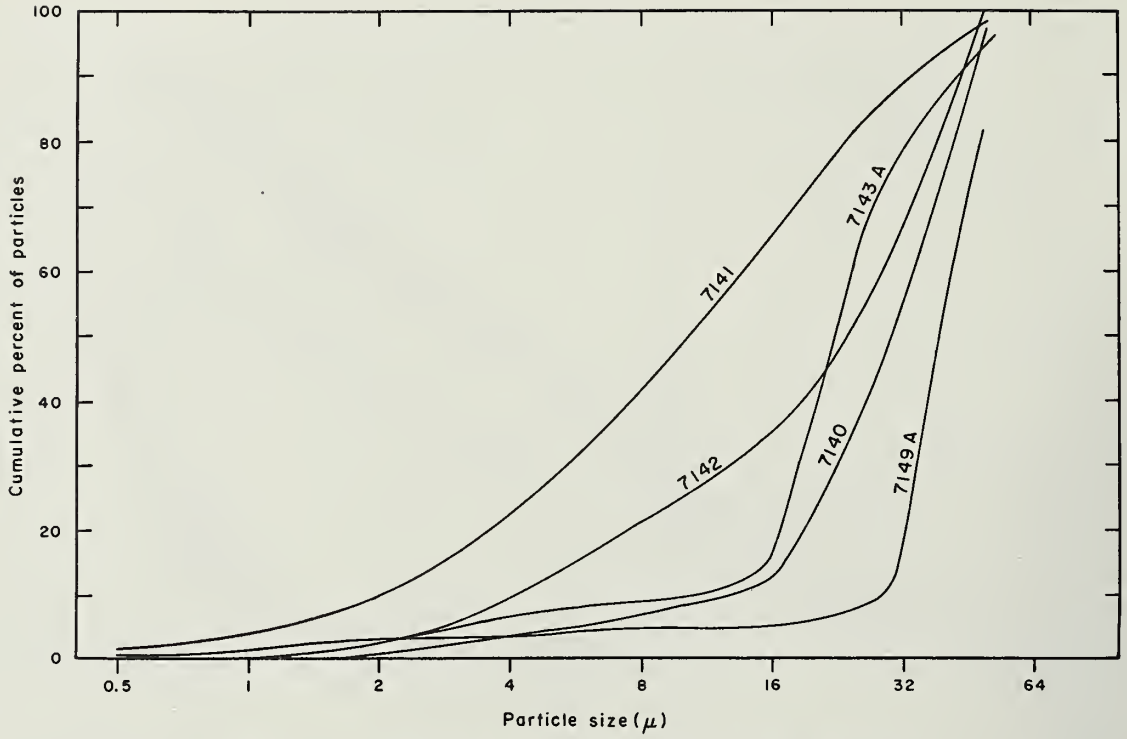

Fig. 5 - Particle-size distribution of marl samples.

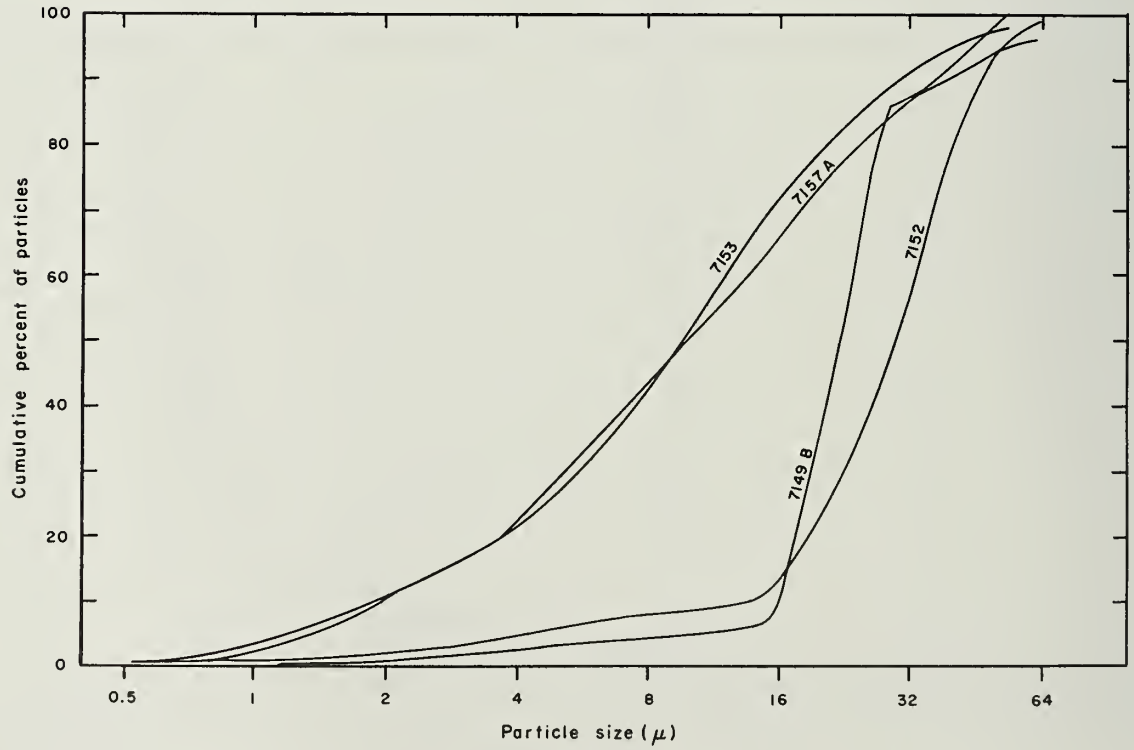

Fig. 6 - Particle-size distribution of marl samples and calcite sludge (7153).

and vigorously stirred for 15 minutes and allowed to settle undisturbed for particle-size analyses. The results of these tests are shown graphically (figs. 3 to 6). Interpolation of the curves at the 50 percent point gives the median particle size listed in table 1. For comparison, the particle-size distributions of three limestones (Types 2, 3, and 4 in Harvey and Steinmetz, 1971) crushed and pulverized for 2.5 hours in a ball mill are shown in figure 3. It is clear that the ball milling of dense limestones does not yield a size distribution as fine as that observed for marls.

Crushed shells are thought to have particle sizes similar to those of crushed limestones. The particle sizes of the coquina samples (fig. 3) are intermediate between those of the pulverized limestones and those of most marls. Some marls, especially the tufaceous marls, have particle-size distributions with median values up to 40 μ. Clearly the stirring did not disperse a sizable fraction of the grains in these samples. The particle-size distribution of the sludge (7153, fig. 6) is very similar to that of the finest marls.

Mineralogical and Chemical Analyses

Portions of the pulverized samples were analyzed for their mineral content by X-ray diffraction. The results are shown in table 2. The major mineral component in most of the samples is calcite, the rhombehedral form of $CaCO_3$. Sample 7121B was collected as a shell sample, but a high proportion of the sample was fine quartz sand. A few other samples contain abundant quartz (sand), which frequently occurs adjacent to, and associated with, deposits of many coquinas and marls. Sample 7123, a quartz sand containing some shells, was collected from the Caloosahatchee Marl in southern Florida. Sample 7153, a carbonate sludge from a paper mill, is more than 95 percent fine-grained calcite and resembles marl in many respects.

Trace and minor minerals in marls (table 2) are quartz (in the form of silt, 4 μ to 30 μ grains); feldspar (silt); aragonite, which occurs in the fossil shells common in marls; dolomite; pyrite; and clay minerals.

Results of chemical analyses of all but the most impure samples are shown in table 3. The sodium oxide (Na_2O) content was determined by neutron activation; K_2O by flame photometry; CO_2, SO_3, and organic carbon by gravimetric analysis; and the remaining oxides by X-ray fluorescence. In addition to those oxides shown (table 3), trace amounts of TiO_2 and MnO were detected in several of the samples. The higher TiO_2 values (between 0.11 and 0.43 percent) were observed in the most silty (quartz) samples. All samples containing less than 20 percent SiO_2 have less than 0.10 percent TiO_2. MnO content was determined on all samples. Sample 7129 contained 0.22 percent. Three samples contained 0.05 to 0.06 percent MnO (7130, 7133, and 7138). All other samples contained less than 0.04 percent MnO. The H_2O+ values were assumed to be the difference between the loss on ignition at 1000° C and the sum of CO_2 and the organic carbon in oven-dried (110° C) samples.

The two columns on the far right in table 3 are values calculated from loss on ignition data and the CaO values. The "CaO in calcine" represents the weight percentage of the CaO in the sample after being heated to 1000° C. The $CaCO_3$ values refer to the oven-dried sample.

TABLE 2 — MINERALOGY OF SAMPLES

Sample number	Major	Minor	Trace
7120	calcite	-	-
7121A	aragonite	calcite	-
7121B	quartz & aragonite	calcite	-
7122A	calcite	quartz	-
7122B	calcite & quartz	aragonite	-
7123	quartz	calcite & dolomite	-
7124	aragonite	-	?
7125	calcite	quartz	-
7126A	calcite	aragonite & quartz	-
7126B	calcite	-	aragonite
7127A	quartz	calcite & clay	feldspar
7127B	quartz	clay	feldspar
7127C	quartz	clay & dolomite	calcite
7127D	calcite	-	-
7128A	calcite	quartz	-
7128B	calcite	-	-
7129	calcite	quartz	-
7130	calcite & quartz	-	dolomite
7131A	calcite	quartz	aragonite & feldspar
7131B	calcite	quartz	feldspar
7131C	quartz & calcite	dolomite & feldspar	clay
7132A	calcite	-	feldspar (?)
7132B	calcite	-	-
7132C	calcite	-	-
7132D	calcite	-	-
7133	calcite	-	-
7134A	calcite	quartz	pyrite
7135	calcite	-	-
7136	calcite & quartz	dolomite	feldspar (?)
7137	calcite	quartz	-
7138	calcite	-	quartz & aragonite
7139	calcite	quartz	-
7140	calcite	-	quartz
7141	calcite	-	quartz, dolomite, & aragonite
7142	calcite	-	quartz & dolomite
7143	calcite	-	aragonite, quartz, & dolomite
7144A	calcite	quartz	dolomite
7145A	calcite	-	quartz
7146A	calcite	quartz	feldspar
7147A	calcite	quartz	-
7148	calcite	gypsum	-
7149A	calcite	-	quartz
7149B	calcite	-	aragonite
7150	calcite	quartz	dolomite & feldspar
7151A	calcite	-	-
7151B	calcite	quartz	dolomite & pyrite
7151C	calcite	-	quartz
7152	calcite	quartz	aragonite
7153	calcite	-	carbon (?)
7154	calcite	quartz	aragonite
7155	calcite	quartz	aragonite
7156	calcite & quartz	-	aragonite & feldspar
7157A	calcite	quartz	aragonite
7157B	calcite	-	quartz, aragonite, & dolomite
7157C	calcite	-	quartz
7157D	calcite	quartz	dolomite
7158	calcite	-	quartz & aragonite
7159	calcite	-	-
7160	calcite & quartz	dolomite	aragonite
7161	quartz	calcite, dolomite, & feldspar	aragonite & clay
7162A	calcite	quartz	aragonite
7162B	calcite	-	quartz, aragonite, & feldspar
7162C	calcite	-	dolomite (?)
7162D	calcite	quartz & aragonite	feldspar (?)
7163A	calcite	aragonite & quartz	dolomite & pyrite
7163B	calcite	aragonite	quartz
7163C	calcite	aragonite & quartz	dolomite
7163D	calcite	quartz & aragonite	dolomite

TABLE 3 — CHEMICAL ANALYSES IN WEIGHT PERCENTAGES
(Analyses by Analytical Chemistry Section, Illinois State Geological Survey)

Sample number	SiO_2	Al_2O_3	Fe_2O_3	MgO	CaO	Na_2O	K_2O	H_2O+	CO_2	SO_3	Organic carbon	CaO in calcine	$CaCO_3$
7120	nil	nil	0.42	0.01	55.5	0.009	0.09	0.08	43.61	0.01	nil	98.6	99.1
7121A	1.36	0.05	0.06	0.13	53.4	0.596	0.09	0.87	41.96	0.07	nil	93.4	95.3
7121B	34.2	nil	0.11	nil	35.4	0.487	nil	nil	28.78	0.11	nil	49.3	63.2
7122A	0.77	nil	0.40	0.91	53.0	0.080	0.02	0.86	42.44	0.09	0.14	93.7	94.6
7122B	22.6	0.70	0.36	0.73	40.5	0.251	0.08	1.33	32.53	0.09	0.09	61.3	72.3
7124	0.88	nil	0.12	0.10	54.0	0.344	0.03	0.92	42.71	nil	nil	95.8	96.4
7125	0.37	0.34	0.49	0.06	53.9	0.407	0.04	0.96	42.50	0.09	nil	95.3	96.2
7126A	2.46	1.09	0.77	1.36	49.4	0.051	0.46	2.03	40.97	0.06	0.96	88.2	88.2
7128B	2.34	1.13	0.27	nil	50.5	0.047	0.12	2.56	39.08	1.74	1.90	89.4	90.1
7129	26.9	5.91	1.57	1.62	38.1	0.147	0.40	2.59	18.24	0.18	2.83	49.9	68.0
7130	40.5	5.79	3.15	2.26	23.3	0.546	1.20	0.03	19.84	0.36	2.53	30.0	41.6
7131B	13.5	2.13	0.89	1.33	40.2	0.331	0.49	2.79	33.15	0.28	3.72	66.6	71.7
7132D	1.21	0.28	0.13	0.03	51.7	0.027	0.05	1.71	40.89	1.20	1.56	92.7	92.3
7133	1.59	0.51	0.16	0.53	51.5	0.041	0.10	1.39	40.17	1.70	1.24	90.0	91.9
7134A	4.33	1.08	0.47	0.64	49.01	0.091	0.15	4.22	36.94	0.15	1.65	85.5	87.5
7135	0.28	0.15	0.12	0.38	47.98	0.030	0.04	5.19	36.50	1.48	6.29	92.4	85.7
7137	1.38	0.47	0.40	0.19	52.7	0.019	0.24	1.61	41.09	0.30	0.40	92.6	94.1
7138	0.43	0.23	0.36	1.18	51.3	0.023	0.03	1.88	41.61	0.12	1.74	93.7	91.6
7139	10.6	2.16	1.05	1.16	42.76	0.186	0.34	1.64	34.50	1.97	2.50	69.7	76.4
7140	0.85	0.08	0.25	1.36	50.9	0.025	0.01	1.88	41.78	0.06	1.65	93.1	90.8
7141	1.70	0.89	0.58	1.75	46.2	0.065	0.06	4.14	37.30	0.13	6.82	87.6	82.5
7142	1.40	0.22	0.66	1.27	49.2	0.037	nil	2.93	39.78	0.23	2.99	90.6	87.8
7143A	0.32	0.12	0.49	1.18	51.1	0.025	0.02	2.91	40.40	0.15	2.99	95.2	91.2
7144A	4.85	0.73	0.54	0.99	47.5	0.103	0.06	2.40	37.98	0.13	3.49	84.6	84.8
7145A	1.53	0.44	0.77	1.46	48.03	0.055	0.02	4.17	37.99	0.12	4.30	89.7	85.7
7146A	9.95	1.38	0.95	1.25	41.02	0.166	0.17	5.33	32.45	0.57	5.91	72.8	73.2
7149A	0.41	0.17	0.13	1.69	52.2	0.030	nil	1.25	42.55	0.07	0.64	94.0	93.2
7149B	0.83	0.12	0.17	1.58	50.59	0.030	nil	2.21	41.69	0.18	1.57	92.8	90.3
7150	7.99	0.83	0.47	1.16	46.6	0.054	0.06	1.82	38.24	0.06	1.48	79.7	83.2
7151A	0.55	0.24	0.99	1.01	41.7	0.044	0.02	9.32	31.56	0.55	13.24	90.9	74.4
7151B	2.83	0.19	1.23	1.33	47.69	0.034	nil	3.10	37.56	0.39	4.86	87.5	85.1
7151C	1.80	0.03	0.42	1.38	49.7	0.036	0.01	2.14	40.99	0.19	2.07	90.7	88.7
7152	1.17	0.34	0.20	1.80	50.3	0.036	nil	1.68	41.77	0.08	1.45	91.3	89.8
7153	nil	0.02	0.19	0.52	53.8	0.853	nil	1.76	41.47	0.14	0.41	95.5	96.0
7155	7.82	0.15	0.10	1.33	46.24	0.108	0.10	2.40	37.89	0.05	2.65	81.0	82.5
7156	35.4	4.19	1.09	1.65	26.16	0.048	0.65	3.84	20.99	0.06	4.77	37.2	46.8
7157A	12.9	2.27	0.85	1.08	42.26	0.196	0.27	2.20	34.32	0.03	2.24	69.0	75.5
7158	6.42	0.66	0.65	3.05	44.86	0.164	0.07	3.01	36.95	0.27	2.94	78.6	80.1
7159	8.88	0.77	0.66	2.26	41.0	0.140	0.01	4.03	34.00	0.20	7.89	75.8	73.2
7160	48.7	6.79	2.46	3.69	17.08	0.701	0.99	1.88	16.43	0.12	0.85	21.1	30.5
7161	55.54	6.52	2.83	1.62	12.55	0.890	1.14	4.27	10.67	nil	3.20	15.3	22.4
7162A	17.6	4.54	1.43	1.52	35.8	0.227	0.39	4.17	29.06	0.62	4.45	57.4	63.9
7162B	8.45	1.41	1.48	1.55	40.7	0.129	0.26	5.88	31.88	0.24	6.64	73.2	72.6
7162C	3.43	0.43	0.86	1.07	48.13	0.046	0.07	2.87	39.24	0.16	2.57	87.0	85.8
7162D	22.0	3.72	2.02	1.47	29.98	0.238	0.48	7.75	23.14	0.61	8.50	49.5	53.5
7163A	14.4	1.55	1.13	0.9	40.6	0.25	0.28	3.27	32.84	0.09	3.89	67.7	72.5
7163B	6.74	0.98	1.11	1.07	44.7	0.13	0.21	3.10	36.32	0.35	4.44	79.6	79.8
7163C	10.88	1.87	2.11	2.99	38.8	0.10	0.57	4.07	33.65	0.27	4.00	66.6	69.3
7163D	12.39	1.86	1.29	1.81	40.3	0.11	0.53	2.78	33.10	1.07	4.34	67.3	71.9

For the marls, the silica (SiO_2) content ranges from nil to 55.6 percent. Approximately half the samples of marls have less that 8 percent silica. Alumina values in the marls range from 0.03 to 6.79 percent. Of 38 samples of marl analyzed, 23 contain less than 0.89 percent Al_2O_3. It is estimated that one-fourth to three-fourths of the alumina occurs in silt-size feldspar grains and that the remaining trace amounts are in clay minerals. The shells and coquinas, except for samples 7121B and 7122B, are high-purity $CaCO_3$. Few marls contain more than 0.15 percent Na_2O, but most of the shells and coquinas test 0.25 to 0.6 percent Na_2O. Most marls test from 1 to 6 percent organic carbon, but one sample (7151A) had more than 13 percent.

Moisture-Density Relations of Marls

To evaluate the possibility of successfully predicting the pore structure and surface area of calcines of marl and/or other important properties related to the reactivity of marls with SO_2, a standard density test was deemed important. Because marls are fine-grained and have soil-like properties and most marl deposits under exploitation contain about 50 percent water before being excavated, a moisture-density relations test (commonly called the "Standard Proctor Test") was thought to be useful. Because of the small quantity of sample available, the miniaturized Proctor test—the Harvard compaction test (Wilson, 1970)—was selected and was run on most of the marls. The results are listed in table 4. The optimum dry density and corresponding moisture content were taken from the maximum point of a density versus moisture curve determined for each sample. Preliminary evaluation of these results indicate that samples with low density have high pore volumes and high organic carbon and H_2O contents.

TABLE 4 — HARVARD MINIATURE COMPACTION TEST RESULTS

Sample	Optimum density (lb/ft^3)	Moisture content (%)
7122B	110	18
7132D	75	38
7133	73	36
7134A	73	44
7137	98	24
7140	73	41
7141	62	53
7142	64	53
7144A	65	51
7145A	57	60
7146A	57	58
7149B	67	48
7150	78	38
7153	77	38
7157A	77	38
7158	62	57
7159	60	54
7163C	60	56

PORE STRUCTURE* AND SURFACE AREA OF SAMPLES AND THEIR CALCINES

Experimental Methods

Mercury Porosimetry

The mercury porosimeter being used in these studies is a 15,000 psi Model 5-7121 from American Instrument Company. The 15,000 psi pressure limit corresponds to penetration of mercury into pores 0.012 μ (1.2×10^{-6} cm) in diameter or greater. The instrument measures the volume of mercury that penetrates voids between particles and pores within particles as a function of pressure. With this instrument the total penetration volume, equal to the total pore and void volume, must be less than 0.2 cc. Because none of the samples thus far tested appears to have many pores smaller than the lower limit, the instrument has proved to be very satisfactory for use in the present studies.

The translation of penetration volume versus pressure data into penetration volume versus pore and void diameter data requires that two important parameters be known. They are the shape of the pores and voids and the contact angle between the mercury-material interface. In most mercury porosimeter measurements it is assumed that the pores and voids are cylindrical in shape and that, on the basis of experimental evidence, the contact angle is 130°. The pressure readings are converted into the corresponding pore (or void) diameter, which is then plotted against the measured penetration volume. The resulting plot is a penetration-volume curve that can be used to evaluate the void volume, the total pore volume, and the mean size of the true pores.

The interpretation of a penetration-volume curve obtained for a single particle of material (fig. 7a) is usually simple. Because no voids can be associated with the single particle of material, the penetration-volume curve is the pore-volume curve and, provided that all pores have been reached, the measured total penetration volume is equal to the total pore volume of the material. However, the observed pore-volume curve may not be the true pore-volume curve. If the material contains rather large interior cavities connected to the surface by narrow pores (usually called "ink bottle" pores), the cavities will not be filled until the narrow pores can be penetrated and, hence, the true pore-volume curve will not be observed. The comparison of the pore-volume curve for the single particle with the penetration-volume curves for other particle-size fractions of the material can indicate whether or not "ink bottle" pores are present.

In the present study, as in most studies, it was more desirable to use a large number of particles rather than a single particle in the pore-structure measurements. The mesh sizes of particles chosen were 16x18 (1200 μ

* The term pore structure as used in this report includes the properties of pore volume, porosity, and pore-volume distribution.

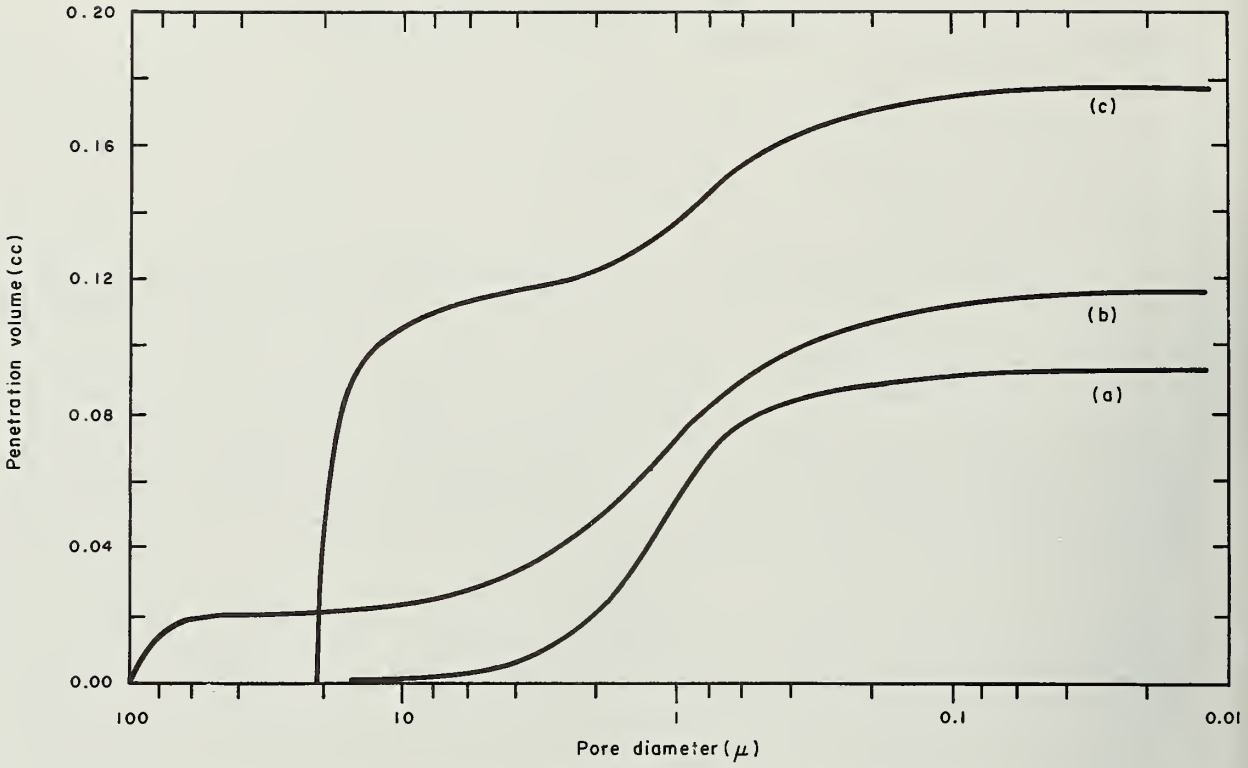

Fig. 7 - Examples of penetration-volume curves for (a) a single particle, (b) 16x18 mesh particles, and (c) 170x200 mesh particles of marl.

to 1000 μ), 40x50 (420 μ to 300 μ), and 170x200 (98 μ to 74 μ). All mesh sizes are U.S. Standard. Most of the measurements have been made on the 16x18 mesh fraction. Although in the "limestone-injection" SO_2 removal process actual use of the marls, chalks, and shells now being studied would probably require the material to be ground to pass 170 mesh (88 μ), it will be seen that pore structure created by calcination is nearly the same for 170x200 mesh particles as for 16x18 mesh particles. However, it should be pointed out that the total pore volume obtained for the 16x18 mesh fraction of a marl or chalk cannot be used simply to represent the total pore volume available in any smaller size fraction of the same material. Because of the polygranular nature of these particles, subdivision of a large particle will take place principally along pores, thereby reducing the total pore volume within the resulting particles. The lost pore volume would be converted into additional void volume between particles.

A major problem in correct interpretation of porosimetry data is to distinguish between void volume and actual pore volume. Any agglomeration of small particles will create a considerable number of interparticle voids, and unless the amount of mercury intrusion into the voids can be determined, the pore-volume measurement will be erroneously high. The penetration of mercury into the voids between packed spheres is characterized by a rather abrupt breakthrough pressure corresponding to the apparent pore diameter of the voids followed by gradual filling of the toroidal voids around the contacting particles.

At the beginning of the present study, penetration-volume measurements were made on nonporous Iceland spar (pure calcite, density 2.71 g/cc) to enable corrections to be made on the observed penetration values of marls and other samples for interparticle void space and other factors such as mercury compressibility. These data showed that 90+ percent of the void space for 16x18 mesh spar was filled at the initial pressure of 1.8 psia (pounds per square inch absolute) and that the remaining void space was filled in the 1.8 to 12 psia range, corresponding to the 100 μ to 15 μ pore-size range. A small amount of additional penetration volume was measured in the 12 to 15,015 psia range (15 μ to 0.012 μ pore-size range). The penetration-volume data for Iceland spar were used to correct other penetration-volume data. A typical penetration-volume curve for 16x18 mesh particles of marl is shown in figure 7b. The first step in the curve represents the filling of voids, and the second step represents the filling of pores within the particles.

For 170x200 mesh particles of nonporous calcite most of the voids are filled at 12 psia (15 μ pores), but they are not completely filled until 200 psia (0.9 μ pores) is reached. These data were used as a zero-pore base line in determining the true pore volume of the 170x200 mesh samples tested. A typical penetration-volume curve for 170x200 mesh particles of marl is shown in figure 7c. The large first step represents the filling of voids, and the second step represents the filling of pores within the particles. Hence, pores much larger than 10 μ in 100 μ particles cannot be distinguished from voids. In practice, voids larger than 15 μ (12 psia) were filled with mercury before any data were recorded.

Calcination

A schematic diagram of the apparatus used for calcination of the carbonate rocks tested in the present study and for subsequent measurements of the surface areas of the calcines is shown in figure 8. The U-shaped sample holder is made from platinum-5 percent rhodium tubing and is connected to the apparatus with Swagelok "quick connect" fittings, which are cooled by an air stream during calcinations. The furnace, capable of reaching 1000° C, can be quickly raised to, or lowered from, position around the sample holder. Calcination takes place under dynamic gas flow conditions and the process is monitored by recording the output of the thermal conductivity cell. The recorder is equipped with a Disc integrator for the measurement of the area under recorder traces. The apparatus and procedures are similar to those used by Thomas and Frost (1971).

Calcination Conditions

The samples tested in the present study were calcined at 850° C under a nitrogen flow rate of 100 cc/min. The calcination time* was less than 14 minutes. Calcines of limestones and dolomites (unpublished data of Frost and

* The term calcination time as used in this report refers to the total time a sample was held at a given temperature even though the actual time required for thermal decomposition (calcination) of the carbonate sample may be considerably less than the total calcination time.

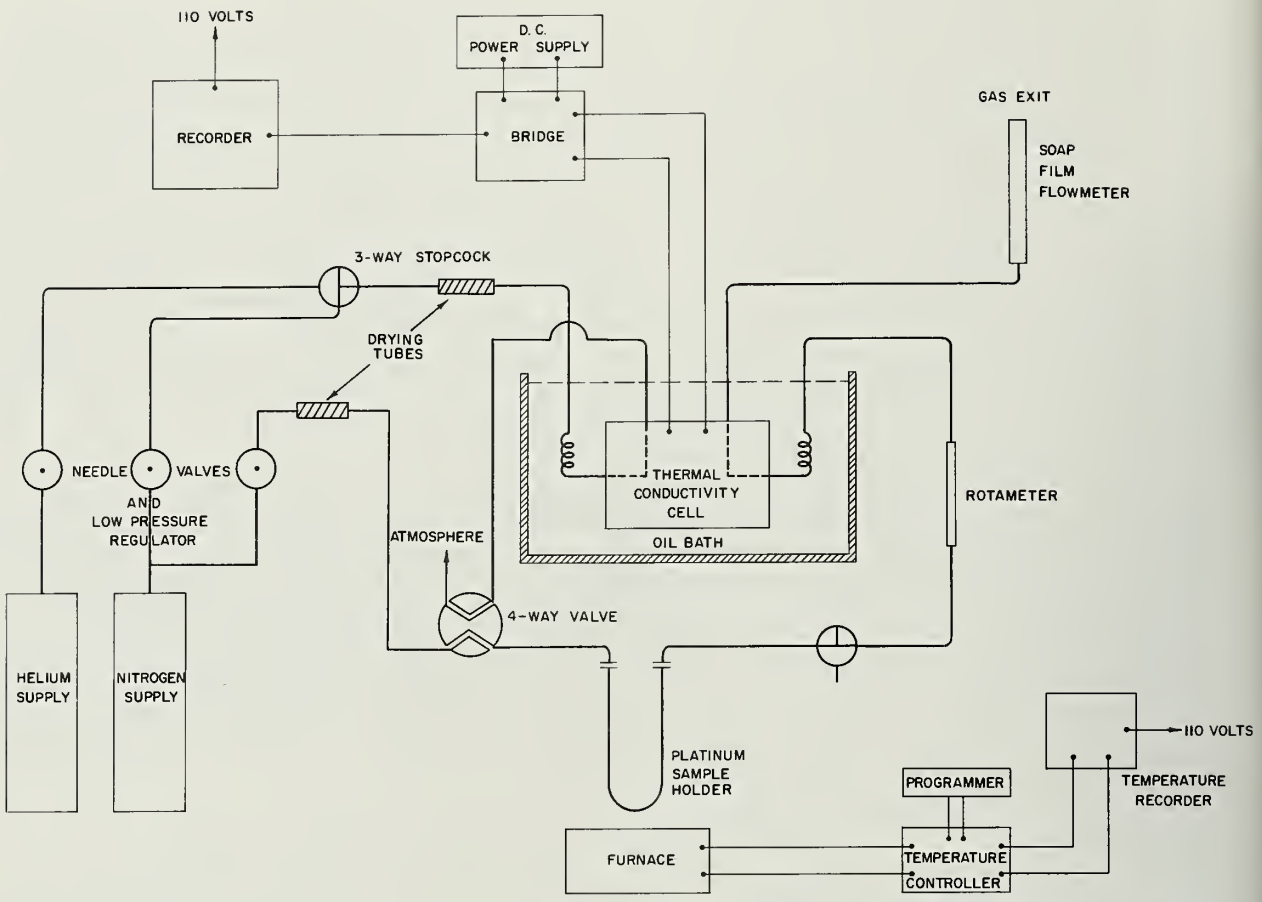

Fig. 8 - Schematic diagram of apparatus used for calcination and measurement of calcine surface area (after Thomas and Frost, 1972).

Thomas) produced under these conditions have high surface areas (20+ m^2/g calcine) and contain fine pores less than 0.2 μ in diameter. Similar properties have been reported by Coutant et al. (1971) for dispersed-phase reactor studies with calcination times of 2 seconds or less. The fine pores created by calcination of marls under the conditions mentioned are thus smaller than those existing in the uncalcined marls. Therefore, interpretation of the pore-volume data is simplified. According to D. C. Drehmel (personal communication, 1971), calcination of three marls at 980° C, under comparatively less dynamic gas flow conditions than those used in this study, produced calcines with much lower surface areas (1.6 to 3.9 m^2/g calcine).

Selected marl samples were calcined at 950° C under a nitrogen flow rate of 100 cc/min to study the effect of calcination temperature on calcine pore structure and surface area. Calcination times were less than 6 minutes. Three marls (7133, 7150, and 7162C) were calcined at 950° C under a 10 percent carbon dioxide-90 percent nitrogen (by volume) gas stream at 100 cc/min. A calcination time of 10 minutes was used, but calcination was complete in less than 5 minutes. The three marls were also calcined at 950° C for 60 minutes under both the pure nitrogen and the 10 percent carbon dioxide-90 percent nitrogen gas streams.

Surface Area Measurements

The use of a flow system (fig. 8) for surface area measurements was first described by Nelsen and Eggertsen (1958). For these measurements, the 3-way stopcock and the 4-way valve are rotated 90 degrees from the positions shown on figure 8. A known mixture of helium and nitrogen is passed over the sample. A dewar flask of liquid nitrogen is raised around the sample holder to greatly lower the temperature of the sample, thereby causing nitrogen to be adsorbed from the flowing gas stream. After about 10 minutes, the dewar of liquid nitrogen is removed, the sample is quickly warmed to room temperature, and the adsorbed nitrogen is then desorbed from the sample. The desorbing nitrogen gives a standard type gas chromatograph peak, which is recorded, and the area under the peak is determined by the Disc integrator. From previously prepared calibration curves, the amount of nitrogen adsorbed is determined. The composition of the gas mixture (determined from gas flow rates) defines the nitrogen adsorption pressure. The flow rate of nitrogen can then be changed to measure the amount adsorbed at other nitrogen pressures. The classical BET (Brunauer, Emmet, and Teller, 1938) equation is then used to calculate the actual surface area. In the present study, the calcine surface areas were calculated from a single adsorption point.

Experimental Procedure

A 0.2 to 0.3 g carbonate sample is weighed and placed in the sample holder, which is then connected to the apparatus. When a stable output signal from the thermal conductivity cell is observed on the recorder, the furnace (preheated to 850° C or 950° C) is raised over the sample holder. The calcination process is completed in 4 to 12 minutes and is monitored on the recorder. About 2 minutes after the apparent completion of calcination, the furnace is removed. The sample holder cools rapidly to room temperature. The calcine surface area is then measured. The calcine sample is removed from the sample holder, weighed, and transferred to a mercury-penetration cell for the pore-structure measurements.

Results and Discussion

Pore Structure of Samples

For a majority of the samples, only the 16x18 mesh size fraction of particles was tested. However, for selected samples, other size fractions also were tested. The pore-structure data are summarized in table 5.

The mean pore size (table 5) was determined from the pore-volume curve by computing the mean of the pore sizes evaluated at the 16th, 50th, and 84th percentiles of the distribution. This procedure more adequately characterizes the central tendency of the distribution than does the 50th percentile alone (Folk, 1958). Likewise, the standard deviation (S.D.) was computed from the pore sizes (S_i) evaluated at the 5th, 16th, 84th, and 95th percentiles by means of

$$S.D. = \frac{S_{95} - S_5}{6.6} - \frac{S_{84} - S_{16}}{4} .$$

TABLE 5 — PORE VOLUME AND MEAN PORE SIZE

Sample number	Mesh size (U.S.)	Pore volume (cc/g)	Mean pore size (μ)	Standard deviation (μ)
7120	+16	0.0825	2.07	0.095
7120	16x18	0.0860	0.50	0.13
7121A	16x18	0.0065	0.30*	
7121B	16x18	0.0125	0.30*	
7122A	16x18	0.0430	0.21	0.13
7122B	+10	0.1065	0.61	0.095
7122B	16x18	0.0840	0.41	0.13
7124	16x18	0.0145	0.15*	
7125	16x18	0.0230	0.20*	
7126A	16x18	0.2325	1.65	0.09
7126A	170x200	0.1500	0.60*	
7126B	16x18	0.3720	5.80	0.13
7127A	16x18	0.1740	0.43	0.16
7127B	16x18	0.1235	0.16	0.16
7127C	16x18	0.1375	0.16	0.16
7127D	3 pieces	0.2880	4.21	0.12
7127D	16x18	0.2505	1.43	0.19
7128A	16x18	0.1990	1.51	0.15
7128B	16x18	0.2080	1.43	0.20
7128B	170x200	0.2000	1.00*	
7129	16x18	0.1385	1.38	0.17
7129	170x200	0.2100	0.60*	
7130	16x18	0.2735	0.81	0.37
7131A	16x18	0.5745	0.50	0.45
7131B	16x18	0.5700	0.57	0.33
7131C	16x18	0.2335	0.35	0.28
7132A	40x50	0.4535	0.84	0.38
7132B	40x50	0.3995	3.45	0.22
7132C	16x18	0.4865	0.87	0.26
7132D	1 piece	0.4667	0.58	0.28
7132D	16x18	0.3805	0.86	0.24
7132D	170x200	0.5680	2.00*	
7133	1 piece	0.3904	3.13	0.23
7133	16x18	0.3150	4.44	0.15
7133	170x200	0.0700	1.00*	
7134A	16x18	0.4905	1.21	0.42
7135	16x18	0.5740	1.63	0.18
7137	16x18	0.2770	0.47	0.23
7138	16x18	0.5440	1.28	0.27
7139	16x18	0.5225	1.31	0.37
7140	16x18	0.4840	1.34	0.34
7141	16x18	0.6725	1.72	0.22
7142	16x18	0.5505	1.22	0.38
7143A	16x18	0.5750	1.68	0.18
7144A	16x18	0.5545	1.27	0.36
7145A	16x18	0.6250	1.07	0.27
7146A	16x18	0.5435	0.69	0.26
7147A	16x18	0.6189	1.12	0.31
7148	16x18	0.1260	4.26	0.11
7149A	16x18	0.4099	4.85	0.14
7149B	16x18	0.5808	2.14	0.21
7150	1 piece	0.4658	1.25	0.45
7150	16x18	0.4724	1.30	0.24
7150	170x200	0.2500	0.80*	
7151A	16x18	0.5997	2.58	0.23
7151B	16x18	0.5732	1.15	0.33
7151C	16x18	0.4460	0.78	0.51
7152	16x18	0.3995	1.07	0.32
7153	170x200	0.2700	1.50*	
7154	16x18	0.6390	3.22	0.17
7155	16x18	0.4205	2.25	0.15
7156	16x18	0.4580	1.93	0.24
7157A	16x18	0.3670	1.38	0.29
7157B	16x18	0.3580	0.60	0.42
7157C	16x18	0.5000	0.90	0.38
7157D	16x18	0.4005	0.70	0.29
7158	16x18	0.5045	1.02	0.26
7159	16x18	0.6220	1.28	0.33
7160	16x18	0.2190	2.06	0.16
7161	16x18	0.2135	0.83	0.26
7162A	1 piece	0.7942	5.65	0.22
7162A	16x18	0.5125	2.98	0.15
7162A	170x200	0.3200	1.50*	
7162B	16x18	1.0780	3.98	0.19
7162C	16x18	0.9340	3.10	0.24
7162C	40x50	0.7825	2.66	0.17
7162C	170x200	0.3200	1.50*	
7162D	16x18	0.7450	3.38	0.16
7163A	16x18	0.7750	1.70	0.17
7163C	16x18	0.5910	2.64	0.19
7163C	170x200	0.3400	0.80*	
7163D	3 pieces	0.8311	2.72	0.16
7163D	16x18	0.7190	2.44	0.15

*An estimated mean pore size.

For the 170x200 mesh size fraction of particles and some shell samples, a simple mean pore size was estimated and these values are included in table 5.

16x18 Mesh Particles

The pore volume of a high-purity coquina (sample 7120) is 0.086 cc/g and the pore volume of a low-purity coquina (sample 7122B) is 0.106 cc/g. The shells (samples 7121, 7124, and 7125) have low pore volumes, from 0.006 cc/g to 0.023 cc/g. The pore volumes of the coquinas and shells are all notably less than those of the lake and bog marls, whose values range from 0.21 to 1.08 cc/g, with a majority of the values in the 0.3 to 0.6 cc/g range. The pore volumes of the tufaceous marls are on the low end of the pore-volume range for marls. Variation in pore volume exists for samples of marls taken from the same deposit, especially 7126, 7131, 7151, 7157, and 7162. These differences are probably due to the variations in quartz and organic composition.

The mean pore-size values (0.47 μ to 5.80 μ) vary significantly between the samples tested—in some cases, even between samples from the same deposit. The size of the pores in the marls is rather evenly distributed from 0.1 μ to larger than 10 μ in diameter. The average of the mean pore sizes of the lake and bog marls is 1.7 μ.

170x200 Mesh Particles

With the exception of marls 7129 and 7132D, the pore volume of the 170x200 mesh particles is less than that of the 16x18 mesh particles, as expected. It is possible that the pore volumes listed for 170x200 mesh particles of 7129 and 7132D still contain appreciable void space volume and/or that the pore volumes of the 16x18 mesh particles are low.

The estimated average pore size for the 170x200 mesh particles is less than the mean pore size calculated for the 16x18 mesh particles of the same sample except in sample 7132D. The larger pores (> 15 μ) present in the 16x18 mesh particles shift the mean pore size to higher values, but these large pores are not detected in measurements of the smaller particles.

Sample Calcination

Three typical calcination recorder traces are shown in figure 9. The trace shown in figure 9a is representative of the shells and coquina samples calcined at 850° C. The height of the trace above the base line is proportional to the CO_2 concentration in the gas stream. Hence, the area under the trace is proportional to the CO_2 content of the carbonate sample. There is no readily available explanation for the small dip at the front of the trace. The general shape of the trace suggests a receding shell calcination model.

Traces typical of lake marls and bog marls calcined at 850° C (fig. 9b) have three distinct regions. The large initial negative dip (cut off by a recorder stop) is due to the decomposition of the relatively large quantities of organic matter present in the sample. An appreciable quantity of CO_2 from carbonate decomposition is included in the negative peak, as evidenced by

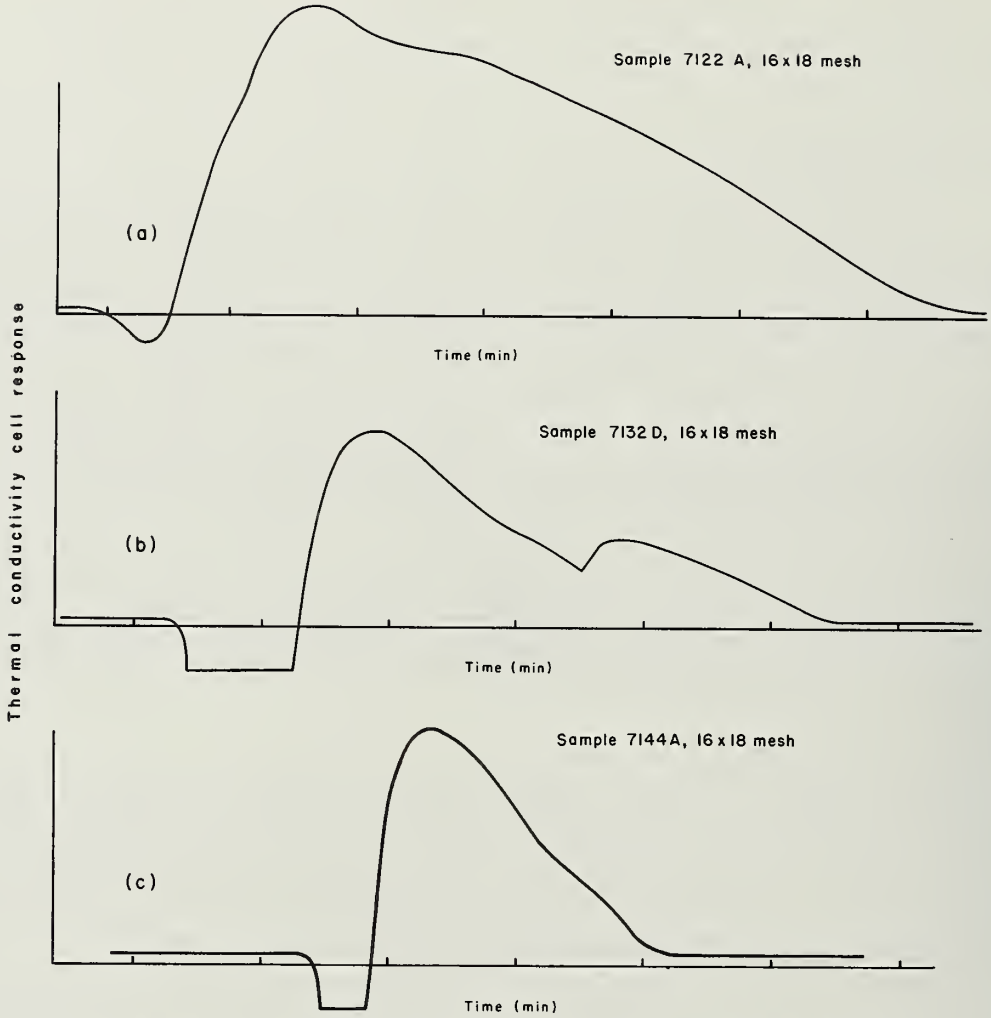

Fig. 9 - Typical calcination recorder traces for (a) shells and coquinas calcined at 850° C, (b) lake and bog marls calcined at 850° C, and (c) lake and bog marls calcined at 950° C.

observed flow rates and time of appearance of the CO_2 peak, and by the considerable loss in the expected integrated area under the positive portion of the calcination trace. A possible explanation for the two distinct positive regions on the observed trace is that they represent decomposition of widely differing size groups of carbonate grains. Since carbonates will not calcine in high concentrations of CO_2, the calcination of the largest grains may be suppressed by the rapid calcination of the very fine grains. It is also possible, because of the charring of the organic carbon, that the suggested grain-size groups are actually one group, and traces like figure 9a, which has a small secondary hump, would be observed if the organic carbon were absent.

The trace shown in figure 9c is typical of the marls calcined at 950° C under both the pure nitrogen and the 10 percent carbon dioxide-90 percent nitrogen gas streams. The effect of the increased temperature on the actual time for complete calcination is readily seen by comparing figures 9b and 9c. The calcination trace at 950° C is characterized by two regions instead of the three observed for calcinations at 850° C. The absence of the third region in the calcination trace (950° C) must be directly related to the

increase in calcination temperature. At 950° C, calcium carbonate will calcine under considerably higher carbon dioxide concentrations than at 850° C. Therefore, at 950° C, the rate of calcination for all carbonate grains present in a marl sample is sufficiently rapid that calcination of the larger grains is not suppressed sufficiently by calcination of the smaller grains to be observed.

Pore Structure of Calcines

A few of the samples, the pore structures of which were determined, were not calcined as part of the calcination tests. The samples eliminated from the calcination test program are of low purity (< 70 percent $CaCO_3$ content), and all contain in excess of 20 percent quartz.

16x18 Mesh Particles

The pore-volume data for both the calcined (850° C) and uncalcined 16x18 mesh fraction of marls and shells are given in table 6. The surface areas of the calcines (850° C) are included in table 6. The calcine (850° C) pore volumes in table 6 were calculated from the weight of uncalcined sample used to prepare the calcine. This procedure simplifies the calculation of the pore volume created by the calcination process. The theoretical pore-volume increase due to calcination, assuming no particle shrinkage and based on the $CaCO_3$ analyses (table 3), was calculated* and is included in table 6. The increase in pore volume on calcination of the samples tested was computed from measured data by two methods. In the first, it was assumed that the increase in pore volume was simply the difference between the total pore volume of the calcined and uncalcined sample. In the second, the increase in pore volume was computed from that portion of the calcine pore-volume curve apparently created by calcination of the $CaCO_3$, i.e., the second step of the pore-volume curve. Characteristic textural features of the calcines are shown in plate 6.

The coquina and shell samples increased in pore volume on calcination at 850° C from 0.156 cc/g rock to 0.215 cc/g rock for the 16x18 mesh particles. Because of the low porosity of the uncalcined samples and the largeness of the pores created by calcination, it was assumed that the pore-volume increase on calcination was equal by either method of computation. The pore-volume increase for the high-purity coquina (7120) of 0.173 cc/g rock is less than the theoretical pore-volume increase of 0.20 cc/g rock. This difference could result from shrinkage of the particles on calcination. The shell samples 7121A, 7122A, 7122B, 7124, and 7125, having very low organic carbon and moderate silica contents, produce a slightly higher than theoretical pore-volume increase on calcination. The pores created by calcination of these samples at 850° C are between 0.25 μ and 2.3 μ in diameter. An electron micrograph of shell sample 7124 calcined at 850° C is shown in plate 6A. The CaO grains, about 1 μ to 4 μ in diameter, are rounded and partly fused. Thus relatively large pores are observed in the shell sample calcine. The texture of the calcine is very similar to that of certain types of limestones calcined at 980° C (Types 3 and 4, Harvey, 1970). The pore-volume curves for the aragonite shell sample (7124) and its calcine (fig. 10) are essentially identical to the curves of calcitic shells

* 1 g pure $CaCO_3 \rightarrow$ 0.56 g CaO. On the basis of densities of 2.71 g/cc for $CaCO_3$ and 3.32 g/cc for CaO, one obtains the theoretical volumes of 0.369 cc/(g of $CaCO_3$) and 0.169 cc/(0.56 g of CaO) and hence, 0.200 cc increase in pore volume when 1 g of pure $CaCO_3$ is calcined.

TABLE 6 — PORE STRUCTURE OF CARBONATE ROCKS AND THEIR CALCINES; SURFACE AREAS OF THE CALCINES

		Carbonate rock - 16x18 mesh particles			Calcine of 16x18 mesh rock particles				
							Pores <0.1μ diameter†		
Sample number	Type	Pore volume (cc/g)	Mean pore size (μ)	Standard deviation (μ)	Pore volume (cc/g rock)	Pore-volume increase* (cc/g rock)	Theoretical pore volume** (cc/g rock)	Pore volume (cc/g rock)	Average pore diameter (μ)	Surface area (m^2/g calcine)
7120	Coquina	0.086	2.07	0.10	0.259	0.173	0.200	0.173	0.045	26.6
7121A	Sea shells	0.006	0.2-0.4	-	0.207	0.201	0.191	0.201	2.3	2.0
7122A	Coquina	0.043	0.21	0.13	0.258	0.215	0.189	0.215	0.25	5.2
7122B		0.106	0.41	0.13	0.262	0.156	0.145	0.156	0.7	3.3
7124	Shells	0.014	0.1-0.2	-	0.221	0.207	0.194	0.207	1.5	0.6
7125	Shells	0.023	0.1-0.2	-	0.240	0.217	0.194	0.217	1.8	0.6
7128B	Tufaceous bog marl	0.208	1.43	0.20	0.410	0.202	0.180	?	0.06	9.3
7131B	Bog marl	0.570	0.57	0.33	0.764	0.194	0.143	0.150	0.045	18.5
7132D	Bog marl	0.380	0.86	0.24	0.638	0.258	0.184	0.155	0.05	21.0
7133	Tufaceous bog marl	0.315	4.44	0.15	0.560	0.245	0.184	0.180	0.07	15.1
7134A	Lake marl	0.490	1.21	0.42	0.650	0.160	0.175	0.150	0.043	22.3
7135	Clayey and peaty marl	0.574	1.63	0.18	0.770	0.196	0.171	0.145	0.05	27.1
7137	Bog marl	0.277	0.47	0.23	0.484	0.207	0.188	?	0.10	9.4
7138	Lake marl	0.544	1.28	0.27	0.788	0.244	0.183	0.150	0.05	20.4
7139	Bog marl	0.522	1.31	0.37	0.668	0.146	0.153	0.120	0.035	21.6
7140	Lake marl	0.484	1.34	0.34	0.716	0.232	0.182	0.165	0.04	26.4
7141	Bog marl	0.672	1.72	0.22	0.844	0.172	0.165	0.135	0.044	26.6
7142	Lake marl	0.550	1.22	0.38	0.739	0.189	0.176	0.150	0.044	21.4
7143A	Bog marl	0.575	1.68	0.18	0.760	0.185	0.182	0.150	0.044	27.0
7144A	Lake marl	0.554	1.27	0.36	0.742	0.188	0.170	0.145	0.04	24.7
7145A	Lake marl	0.625	1.07	0.27	0.886	0.261	0.172	0.110	0.044	23.4
7146A	Lake marl	0.543	0.69	0.26	0.688	0.145	0.146	0.090	0.035	29.7
7149A	Bog marl	0.410	4.85	0.14	0.578	0.168	0.187	0.160	0.04	28.3
7149B		0.581	2.14	0.21	0.816	0.135	0.182	0.145	0.037	26.2
7150	Lake marl	0.472	1.30	0.24	0.560	0.088	0.167	0.140	0.04	22.0
7151A		0.600	2.58	0.23	0.760	0.160	0.149	0.120	0.03	68.8
7151B	Bog marl	0.573	1.51	0.33	0.766	0.193	0.170	0.155	0.04	27.2
7151C		0.446	0.78	0.51	0.619	0.173	0.178	0.170	0.044	22.5
7152	Bog marl	0.400	1.07	0.32	0.610	0.210	0.179	0.160	0.037	28.8
7155	Lake marl	0.420	2.25	0.15	0.678	0.258	0.165	0.130	0.037	22.2
7157A	Lake marl	0.367	1.38	0.29	0.530	0.163	0.155	0.125	0.035	21.2
7158	Lake marl	0.504	1.02	0.26	0.698	0.194	0.161	0.120	0.037	26.8
7159	Bog marl	0.622	1.28	0.33	0.834	0.212	0.147	0.140	0.045	28.7
7162C	Bog marl	0.934	3.1	0.24	1.028	0.094	0.172	0.100	0.04	24.8
7163A		0.775	1.7	0.17	0.894	0.119	0.146	0.110	0.032	25.8
7163C	Bog marl	0.591	2.64	0.19	0.792	0.201	0.139	0.105	0.035	24.4
7163D		0.719	2.44	0.15	0.859	0.140	0.144	0.110	0.035	24.4

*Column 4 minus column 1.

**Based on $CaCO_3$ content of rock sample, assuming no shrinkage of $CaCO_3$ grains on calcination.

†Calculated from the less than 0.1μ portion of the pore volume versus pore size graph.

‡These data within the box were calculated from the entire calcine pore-distribution graph.

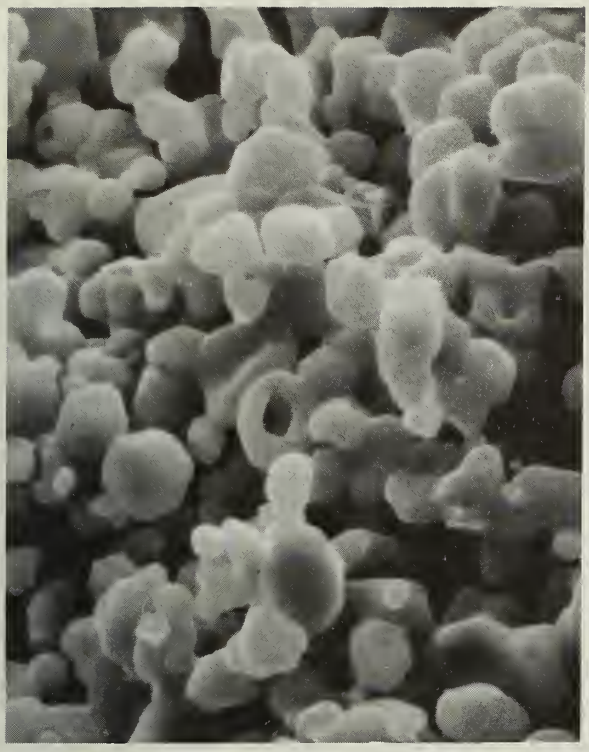

A. Shell 7124 5μ (x3860)

B. Marl 7151A 5μ (x3720)

C. Marl 7150 2μ (x8910)

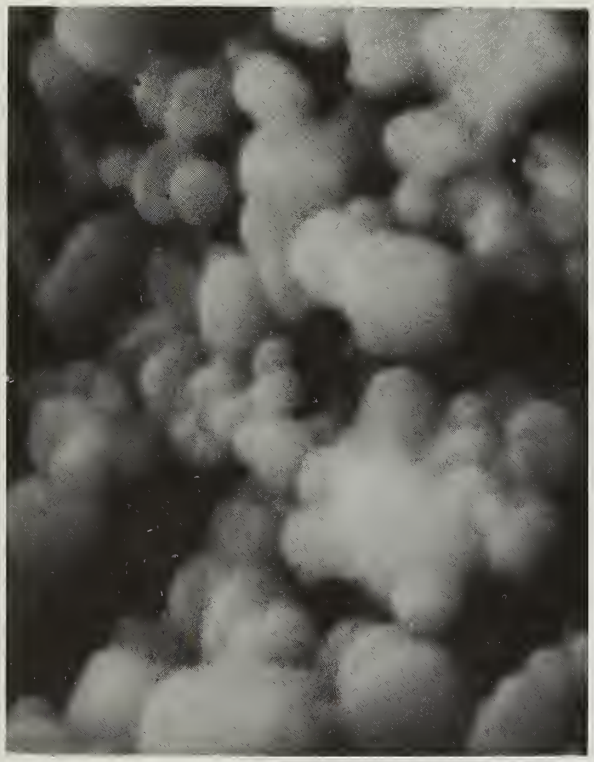

D. Sludge 7153 1μ (x12,400)

Plate 6 - Typical textural features of calcined samples of shell, marl, and a calcitic sludge (waste).

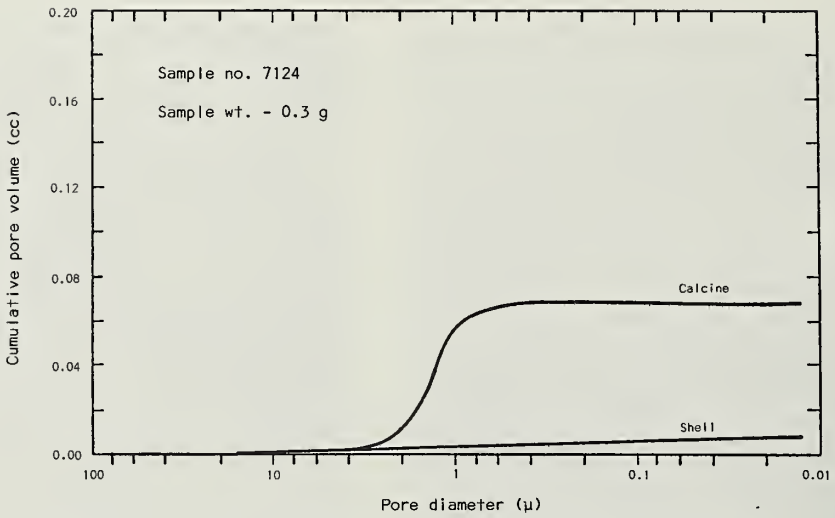

Fig. 10 - Pore-volume curves for 16x18 mesh particles of clam shell 7124 and its calcine.

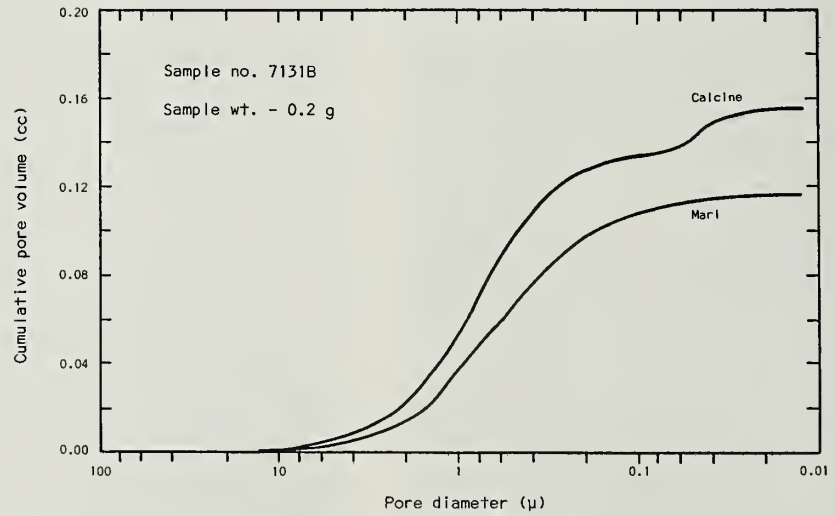

Fig. 11 - Pore-volume curves for 16x18 mesh particles of bog marl 7131B and its calcine.

and indicate that the properties causing low porosity and large pores in calcines of shells are independent of the crystallographic form of the $CaCO_3$.

The pore-volume increase of the marl particles (16x18 mesh), on calcination at 850° C computed from total pore volumes, ranges from 0.094 cc/g marl to 0.261 cc/g marl; in the majority of the samples, the increase is between 0.18 cc/g marl and 0.22 cc/g marl. The pore-volume increase computed from the second step of the calcine pore-volume curve ranges from 0.09 cc/g marl to 0.180 cc/g marl. The theoretical pore-volume increase ranges from 0.143 cc/g marl to 0.188 cc/g marl. A sample-by-sample comparison of the data in table 6 shows that the pore-volume increase determined from total pore volumes is usually higher than theoretical, while all values calculated from the second step of the 850° C calcine pore-volume curves are slightly less than the theoretical values. A majority of the pores created by calcination of the marls at 850° C have diameters of less than 0.1 μ. The times required for calcination of the marl samples are nearly equivalent, suggesting that the $CaCO_3$ grain size does not change appreciably from marl to marl.

Electron micrographs of marls 7151A and 7150 calcined at 850° C are shown in plate 6, B and C. The CaO grains, about 0.2 μ to 0.7 μ in diameter, are aggregated into particles about 2 μ to 7 μ across. These particles are interpreted to have been derived from individual calcite grains (up to 7 μ) in the original marl. The largest pores observed are those existing in the uncalcined marls. The very fine pores (< 1.0 μ in diameter) are within the clusters of the very fine CaO grains.

Discussion of the increase in pore volume of the marls on calcination at 850° C is necessarily complicated by the wide variation of the silica and/or organic carbon content of the marls. The pore-volume values calculated from the calcine pore-volume curves are, and should be, less than the theoretical values since some particle shrinkage on calcination is to be expected. The pore-volume values, calculated from the total pore-volume data, are undoubtedly influenced by the organic carbon content of the marls. It appears that some, or all, of the organic carbon in many of the marl samples occurs between the calcite grains and is at least partially removed during calcination, thus producing pore volume not associated with the calcite decomposition. Figure 11 (7131B) and figure 12 (7132D) are representative of the pore-volume curves obtained from most of the marl samples. While there is a substantial increase in the pore volume of pores greater than 0.1 μ in diameter, the mean pore size appears to remain constant. Marl 7149A has a low organic carbon content, and the pore-volume curves (fig. 13) are almost identical except for the very fine pores (< 0.1 μ) in the calcine. Marl 7137 has a low organic carbon content, but the calcine pore-volume curve (fig. 14) is more distinctly different from the marl pore-volume curve than the differences between corresponding curves shown in figures 11, 12, and 13.

Data are given in table 7 illustrating the effect of different calcination conditions on pore structure of calcined 16x18 mesh marl particles. With the exception of marl 7162C, only small changes in the total calcine pore volume are observed here. An appreciable fraction of the 16x18 mesh particles of marl 7162C disintegrated when calcined at 950° C, thereby decreasing the total pore volume in the calcine. The pore-volume curves for five different calcination conditions are given for marls 7133, 7150, and 7162C in figures 15, 16, and 17. Simply increasing the calcination temperature from 850° C to 950° C

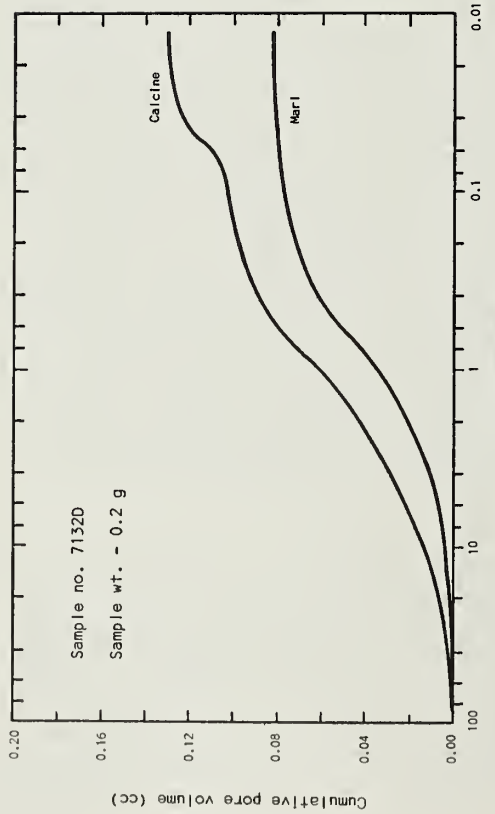

Fig. 12 - Pore-volume curves for 16x18 mesh particles of bog marl 7132D and its calcine.

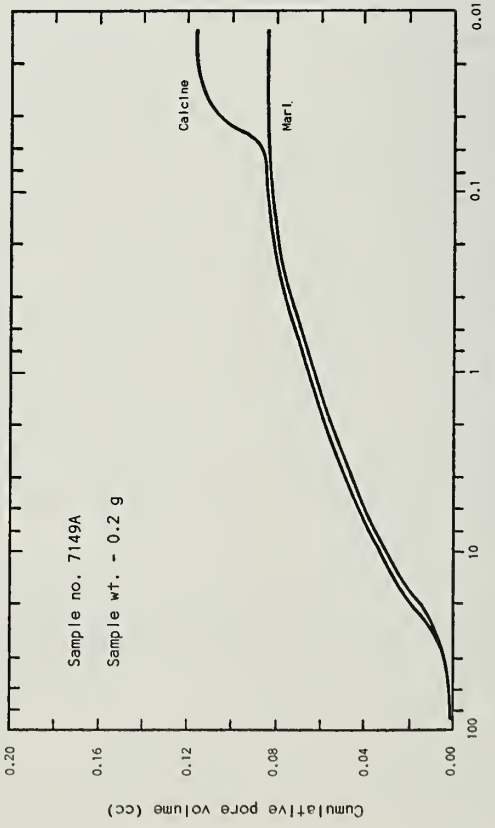

Fig. 13 - Pore-volume curves for 16x18 mesh particles of bog marl 7149A and its calcine.

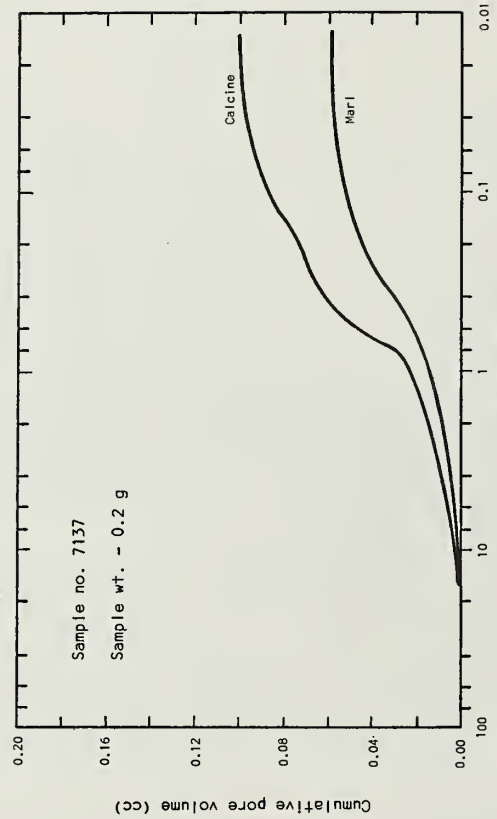

Fig. 14 - Pore-volume curves for 16x18 mesh particles of bog marl 7137 and its calcine.

TABLE 7 — EFFECT OF CALCINATION CONDITIONS ON CALCINE PORE STRUCTURE AND SURFACE AREA OF 16x18 MESH PARTICLES

Sample number	Type	Calcination conditions*	Calcine pore volume (cc/g marl)	Pore volume change on calcination** (cc/g marl)	Average diameter of pores created by calcination (μ)	Surface area (m^2/g calcine)
7132D	Bog marl	(a)	0.638	0.258	0.05	21.0
		(b)	0.646	0.266	0.06	13.7
7144A	Lake marl	(a)	0.742	0.188	0.04	24.7
		(b)	0.723	0.169	0.04	20.8
7145A	Lake marl	(a)	0.886	0.261	0.044	23.4
		(b)	0.755	0.135	0.05	15.3
7149A	Bog marl	(a)	0.578	0.168	0.04	28.3
		(b)	0.588	0.178	0.04	21.6
7133	Tufaceous bog marl	(a)	0.560	0.245	0.07	15.1
		(b)	0.543	0.228	0.08	9.9
		(c)	0.540	0.225	0.13	5.9
		(d)	0.529	0.214	0.10	8.5
		(e)	0.594	0.279	0.30	2.8
7150	Lake marl	(a)	0.560	0.088	0.04	22.0
		(b)	0.544	0.072	0.04	19.0
		(c)	0.587	0.115	0.08	8.0
		(d)	0.513	0.041	0.08	6.3
		(e)	0.523	0.051	0.20	3.1
7162C	Bog marl	(a)	1.028	0.094	0.04	24.8
		(b)	0.948	0.014	0.05	17.7
		(c)	0.892	-0.042	0.13	5.8
		(d)	0.710	-0.224	?	3.4
		(e)	0.758	-0.176	?	2.4

*Calcination conditions are as follows:
(a) 850°C, about 7 min., 100% N_2 stream
(b) 950°C, about 4 min., 100% N_2 stream
(c) 950°C, 10 min., 10% CO_2-90% N_2 stream
(d) 950°C, 60 min., 100% N_2 stream
(e) 950°C, 60 min., 10% CO_2-90% N_2 stream

**Calculated from calcine pore volume and marl pore volume (column 1, table 6).

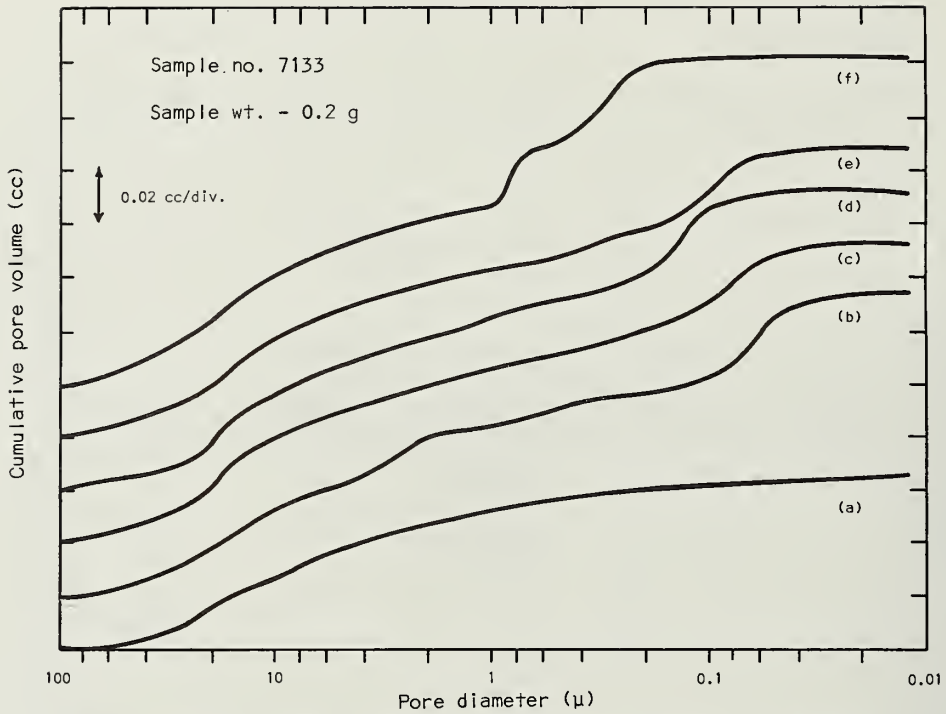

Fig. 15 - Pore-volume curves for 16x18 mesh particles of tufaceous bog marl 7133 (a) and its calcines (b-f). The calcination conditions are: (b) 850° C, about 7 min., 100% N_2 stream; (c) 950° C, about 4 min., 100% N_2 stream, (d) 950° C, 10 min., 10% CO_2-90% N_2 stream; (e) 950° C, 60 min., 100% N_2 stream; (f) 950° C, 60 min., 10% CO_2-90% N_2 stream.

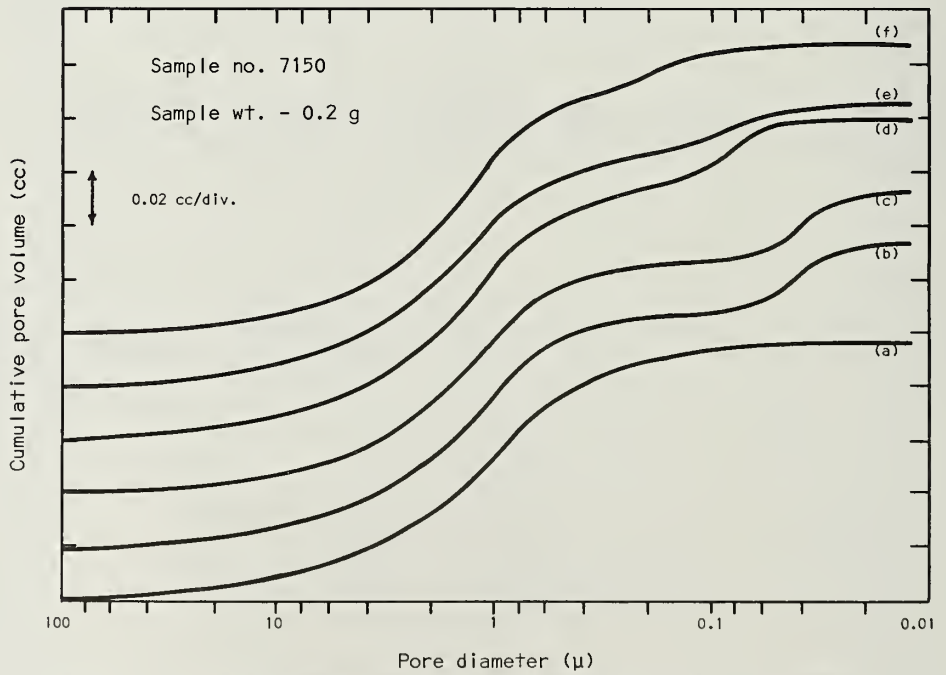

Fig. 16 - Pore-volume curves for 16x18 mesh particles of lake marl 7150 (a) and its calcines (b-f). The calcination conditions are: (b) 850° C, about 7 min., 100% N_2 stream; (c) 950° C, about 4 min., 100% N_2 stream, (d) 950° C, 10 min., 10% CO_2-90% N_2 stream, (e) 950° C, 60 min., 100% N_2 stream, (f) 950° C, 60 min., 10% CO_2-90% N_2 stream.

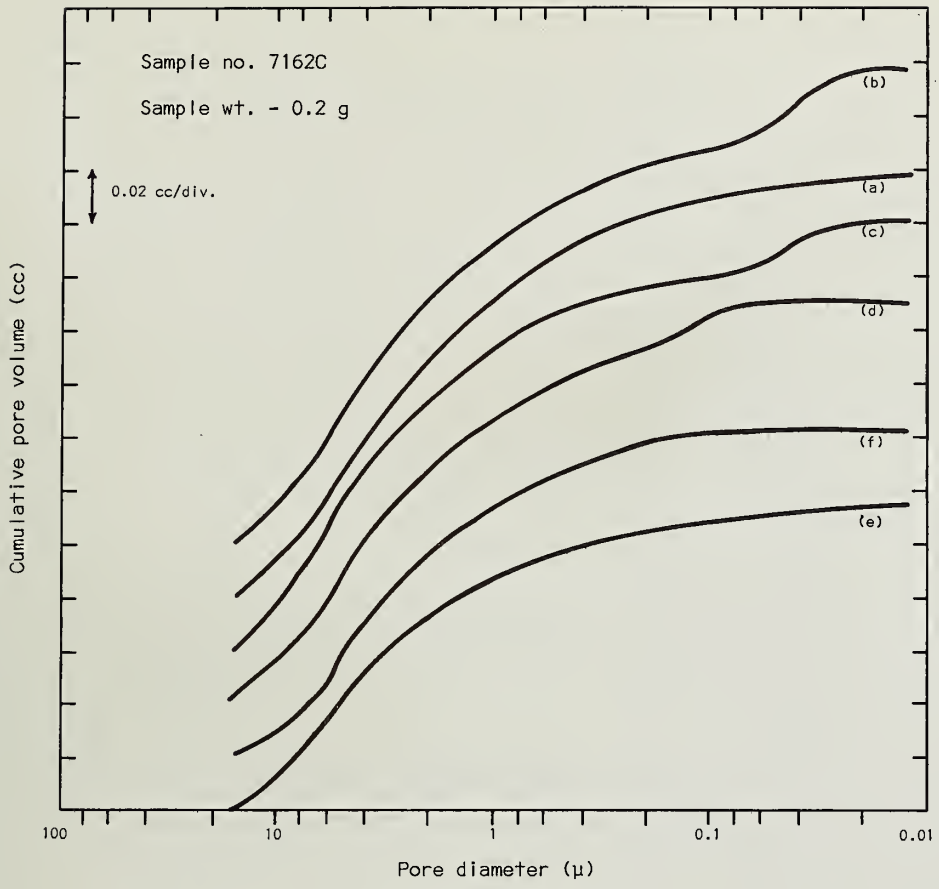

Fig. 17 - Pore-volume curves for 16x18 mesh particles of bog marl 7162C (a) and its calcines (b-f). The calcination conditions are: (b) 850° C, about 7 min., 100% N_2 stream; (c) 950° C, about 4 min., 100% N_2 stream; (d) 950° C, 10 min., 10% CO_2-90% N_2 stream; (e) 950° C, 60 min., 100% N_2 stream; (f) 950° C, 60 min., 10% CO_2-90% N_2 stream.

has only a small, if any, effect on the pore-size distribution. The addition of 10 percent carbon dioxide to the nitrogen gas stream promotes growth of the CaO grains and a corresponding widening of the fine pores created during the calcination process. Longer calcination times of 60 minutes under both the pure nitrogen and the 10 percent carbon dioxide-90 percent nitrogen gas streams usually resulted in further widening of the fine pores. The large pores existing in the marl were usually not affected by either the raising of the calcination temperature to 950° C or the increasing of the total calcination time to 60 minutes.

170x200 Mesh Particles

Table 8 summarizes the data on 170x200 mesh particles of marls calcined at 850° C. Corresponding data from 16x18 mesh particles have been included in table 8. Sample 7153 will be discussed later. Direct comparison of data for marls 7133, 7150, and 7162C shows that the pore structures (< 0.1 μ) of the calcines are not appreciably dependent upon particle size.

Pore-volume and penetration-volume curves for a tufaceous marl (7133, fig. 18) and a lake marl (7150, fig. 19) show the close similarity in shape in the ≤ 0.1 μ pore range for the 16x18 and 170x200 mesh particles and their calcines. Note that for the 170x200 mesh particle data, both the penetration-volume and void-volume curves are shown in figures 18 and 19 to illustrate the

TABLE 8 — COMPARISON OF TEST RESULTS ON 16x18 AND 170x200 MESH PARTICLES

Sample number	Type	Mesh	Carbonate rock		Calcine					
			Pore volume (cc/g)	Average pore size (μ)	Pore volume (cc/g rock)	Pore-volume increase* (cc/g rock)	Theoretical pore volume† (cc/g rock)	Pores <0.1μ diameter** Pore volume (cc/g rock)	Pores <0.1μ diameter** Average pore diameter (μ)	Surface area (m^2/g calcine)
7126A	Bog marl	16x18	0.232	1.65						
7126A		170x200	0.150	0.6	0.320	0.170	0.177	0.180	0.04	25.2
7133	Tufaceous bog marl	16x18	0.315	4.44	0.560	0.245	0.184	0.180	0.07	15.1
7133		170x200	0.070	1.0	0.230	0.170	0.184	0.170	0.055	19.0
7150	Lake marl	16x18	0.472	1.30	0.560	0.188	0.167	0.140	0.04	24.7
7150		170x200	0.250	0.8	0.425	0.175	0.167	0.155	0.045	28.0
7153(1)	Sludge from paper	170x200	0.270	1.5	0.270	0.0	0.192	0.0	?	0.8
7153(2)‡	mfg. plant	170x200	0.270	1.5	0.415	0.145	0.192	0.0	?	
7162C	Bog marl	16x18	0.934	3.1	0.878	0.094	0.172	0.092	0.04	24.8
7162C		170x200	0.320	1.5	0.455	0.135	0.172	0.155	0.045	24.8

*Column 1 minus column 3.

†Based on $CaCO_3$ content of rock sample, assuming no shrinkage of $CaCO_3$ grains on calcination.

**Calculated from the less than 0.1μ portion of the pore volume versus pore size curve.

‡Calcined at 800° C.

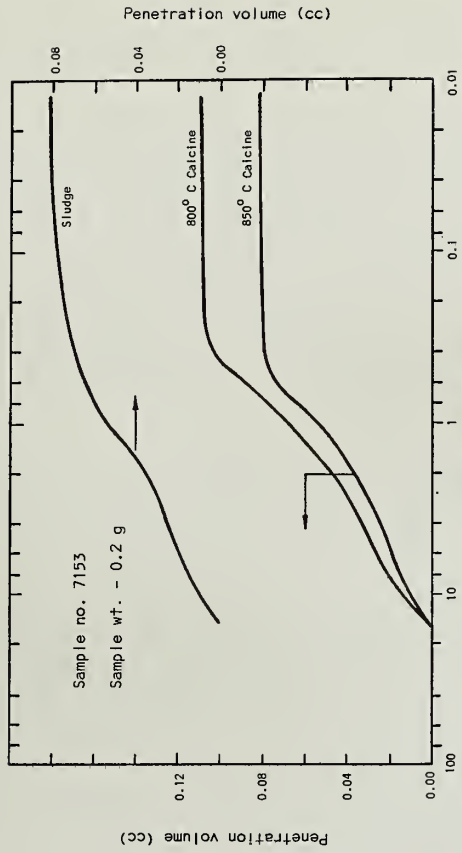

Fig. 20 - Penetration-volume curves for 170x200 mesh particles of carbonate sludge 7153 and its calcines.

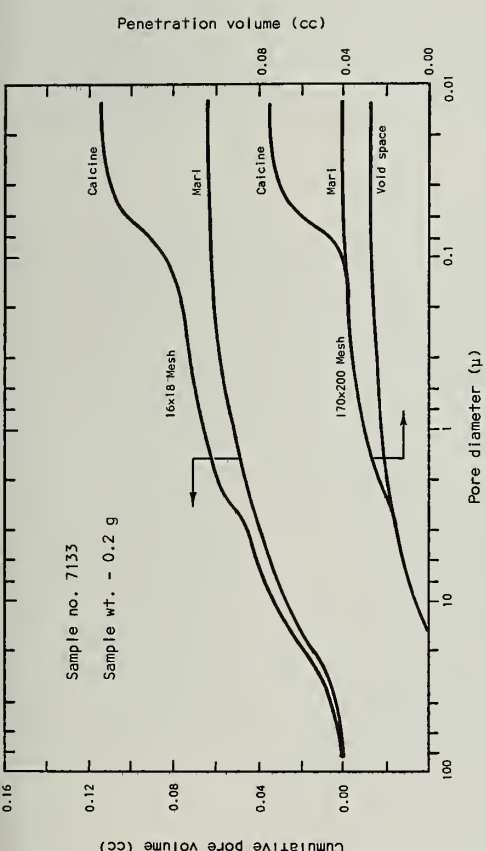

Fig. 18 - Pore-volume curves (left ordinate) for 16x18 mesh particles and penetration-volume curves (right ordinate) for 170x200 mesh particles of tufaceous bog marl 7133 and their calcines.

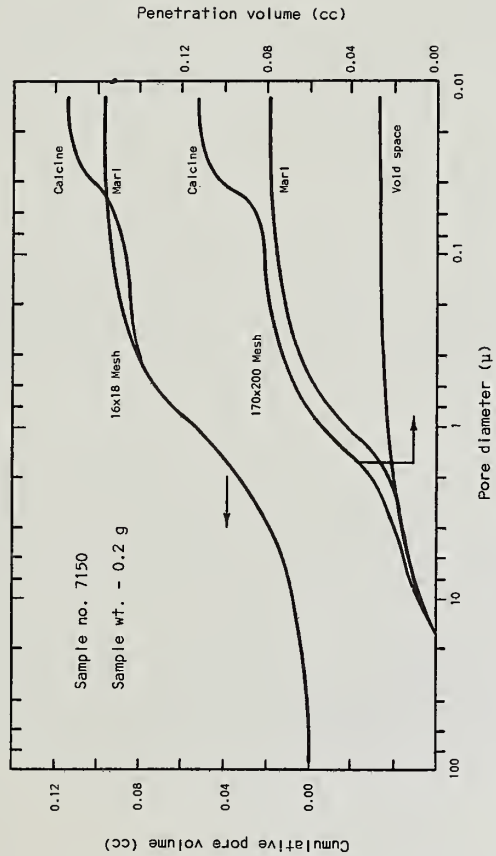

Fig. 19 - Pore-volume curves for 16x18 mesh particles and penetration-volume curves for 170x200 mesh particles of lake marl 7150 and their calcines.

relative importance of the difference between pore volume and penetration volume for these fine-mesh particles. The penetration-volume curve for 170x200 mesh particles of tufaceous bog marl 7133 (fig. 18) is identical with the penetration-volume curve of its calcine in the 2.0 μ to 0.1 μ range, but the penetration-volume curve for 170x200 mesh particles of the lake marl 7150 (fig. 19) lies below the penetration-volume curve of its calcine. However, the pore-volume curve for 16x18 mesh particles of tufaceous bog marl 7133 (fig. 18) lies below the pore-volume curve of its calcine, but the pore-volume curve for 16x18 mesh particles of lake marl 7150 (fig. 19) is identical with the pore-volume curve of its calcine in the 100 μ to 0.4 μ range. It is not clear at this time why these slight differences between the curves are observed. Both figures were included to show some of the complexities in interpreting pore-volume and penetration-volume data.

Sample 7153, a carbonate sludge from a paper manufacturing plant, is of special interest because it is a waste product. Because no 16x18 mesh particles occur in the sample, the 170x200 mesh particles were tested. Sample 7153 was calcined at 800° C and at 850° C. The penetration-volume curves for the calcined and uncalcined samples are similar (fig. 20). The curve for the uncalcined sample has been adjusted upward in figure 20, because it is identical with the 850° C calcine curve except for a small difference in the 0.09 μ to 0.9 μ pore-diameter range. An electron micrograph of the sludge calcined at 850° C is shown in plate 6D. The calcine has some of the same textural features as those seen in the calcined shell sample (pl. 6A). The CaO grains, about 0.3 μ to 2.0 μ in diameter, are spherical and smooth. The $CaCO_3$ grains in the uncalcined sludge are about 0.5 μ to 3 μ in diameter. Since the pore structure of the 850° C calcine and the sludge are nearly identical, it is concluded that shrinkage of the sludge particles took place on calcination. While the shape of the 800° C calcine curve is the same as that of the 850° C curve, it is apparent that there is an increase in the number of pores present in the calcine. Therefore, the lower calcination temperature has simply lowered the rates of the physical processes involved in the calcination of the carbonate and in the growth of the oxide grains.

Surface Areas of Calcines

The surface areas of the 16x18 mesh 850° C calcines are given in table 6. The surface areas of the shell sample calcines are between 0.6 and 5.2 m^2/g calcine. The surface area of a high-purity coquina calcine is 26.6 m^2/g calcine, but the surface area of a low-purity coquina calcine is less than 5 m^2/g calcine. With few exceptions, the surface areas of the marl calcines are between 20 and 30 m^2/g calcine. Generally, the calcines of marls with large amounts of organic matter have the highest surface area values. The very high surface area, 68.8 m^2/g calcine, for the calcine of marl 7151A can be attributed only to its high (13.4 percent) organic carbon content. Thus, some of the carbon remains in the marl calcines after calcination and adds surface area to the sample. The high surface areas of the marl calcines and the low surface areas of the shell sample calcines indicate that the crystallites of CaO formed from the marl are much smaller than those formed from the shells. This is confirmed by microscopy (pl. 6, A, B, and C). The size of the CaO crystallites in the calcines may be influenced by crystal lattice impurities in the $CaCO_3$, which may act as nucleating agents for the formation and growth of CaO grains, and/or by lattice vacancies in the

$CaCO_3$, which may act to cause accelerated sintering upon calcination. If lattice impurities and vacancies act as described, they are more abundant in the shells than in the marls.*

The effect of different calcination conditions on the calcine surface area of 16x18 mesh particles can be seen in table 7. Calcination at 950° C under pure nitrogen lowers the surface areas of the calcines 10 to 40 percent from the values at 850° C. Calcination under a 10 percent carbon dioxide-90 percent nitrogen gas stream lowers the surface areas of the calcines even more. Further reduction in the surface areas of the calcines is observed for calcination times of 60 minutes at 950° C under either the pure nitrogen or the 10 percent carbon dioxide-90 percent nitrogen gas streams. The surface area values obtained at 950° C were generally between 3.0 and 15.0 m^2/g calcine and those obtained at 850° C were between 15.1 and 28.3 m^2/g calcine. However, inspection of these results in table 7 shows that the addition of 10 percent carbon dioxide to the gas stream has a much greater effect on the surface areas of the calcines than simply raising the calcination temperature from 850° C to 950° C.

Only a limited amount of data is available for comparison of surface area values for 16x18 mesh and 170x200 mesh particles of marl calcined at 850° C. The data in table 8 show that the surface areas of the calcines are not very dependent upon particle size.

CONCLUSIONS

Many rocks described in geologic literature as marls are not carbonate rocks, and some are very impure carbonates, which would not be suitable for use in SO_2 control processes. This is especially true of many so-called marls of marine origin, which contain some carbonate constituents, mainly shells and shell fragments, but consist mostly of quartz and clay minerals.

Most deposits of marl (the term marl being restricted to incoherent carbonate-rich sediments of fresh-water origin) have $CaCO_3$ contents between 80 and 90 percent; a few have more than 90 percent. The main impurities are quartz silt and organic matter. The grain (crystallite) size of marls is uniformly fine, with an average mean chord length of approximately 3 μ. Dispersion of marls in water yields median particle sizes varying from 6 μ to 38 μ. These particle sizes are less than half of those of three pulverized (2½ hours in a ball mill) limestones tested.

The pore volume in marl contributes more than 80 percent of the total pore volume in calcined marl. Upon calcination (at 850° C, for 5 to 10 minutes, and under a high gas flow rate), the marl pore structure is retained and the fine pores created are, for the most part, less than 0.1 μ in diameter. The surface areas of the calcines of marls are generally between 20 and 30 m^2/g calcine.

---

* In past studies at the Illinois State Geological Survey, reagent-grade precipitated $CaCO_3$ (1 μ to 2 μ crystals) and Iceland spar (about 1 μ crystals) have been calcined under the same conditions as those used in the present tests. The calcine surface areas are less than 1 m^2/g calcine from the precipitated $CaCO_3$ and about 30 m^2/g calcine from the Iceland spar.

Increasing the calcination temperature to 950° C has little effect on the calcine pore structure but causes some decrease in the surface areas of the calcines. However, calcination at 950° C under a 10 percent carbon dioxide-90 percent nitrogen gas stream and/or for a calcination time of 60 minutes generally enlarges the fine pores. Under these conditions, a major reduction in the surface areas of the calcines is observed.

The pore volume of the coquina and the shells is lower than that of the marls. In contrast to marls, the major portion of the pore volume of the calcined coquina and shell samples is created during their calcination. The shell samples also have larger grain sizes than do the marls. However, a weathered and porous chalky coquina containing porous shells (the Crystal River Formation, 7120) has grain-size and calcined surface area values similar to those of the marls.

The high pore volume and fine grain size of lake marls and their calcines indicates (on the basis of the results of Coutant et al., 1971, and Drehmel, 1971) that the marls have higher reactivities with SO_2 than do coquinas and shells and their calcines.

REFERENCES

Attig, R. C., and P. Sedor, 1970, Additive injection for sulfur dioxide control, a pilot plant study (Research Center Rept. 5460-Contract PH 86-67-127): Alliance, OH, Babcock & Wilcox Co., 59 p. + 7 app.

Borgwardt, R. H., 1970, Isothermal reactivity of selected calcined limestones with SO_2, in Natl. Air Pollution Control Agency Limestone Injection Process Symposium Proc., Gilbertsville, KY, June 22-26.

Brunauer, S., P. H. Emmet, and E. Teller, 1938, Adsorption of gases in multimolecular layers: Jour. Am. Chem. Soc., v. 60, p. 309-319.

Coutant, R. W., et al., 1971, Investigation of the reactivity of limestone and dolomite for capturing SO_2 from flue gas (Final Report-Contract CPA 70-111): Columbus, OH, Battelle, 54 p. + 4 app.

Davis, C. A., 1901, A second contribution to the natural history of marl: Jour. Geology, v. 9, no. 6, p. 491-506.

Dibbs, H. P., 1971, Methods for the removal of sulfur dioxide from waste gases: Canada Dept. Energy Mines and Resources Mines Branch Info. Circ. IC 272, Ottawa, 174 p.

Drehmel, D. C., 1971, Limestone types for flue gas scrubbing, in Second Int. Lime/Limestone Wet Scrubbing Symposium Proc., New Orleans, LA, Nov. 8-12.

Folk, R. L., 1958, Petrology of sedimentary rocks, 2nd ed.: Austin, TX, Hemphill's, p. 47-49.

Harvey, R. D., 1970, Petrographic and mineralogical characteristics of carbonate rocks related to sorption of sulfur oxides in flue gases: Illinois Geol. Survey Environmental Geology Note 38, 31 p.

Harvey, R. D., and J. C. Steinmetz, 1971, Petrographic properties of carbonate rocks related to their sorption of sulfur dioxide: Illinois Geol. Survey Environmental Geology Note 50, 37 p.

Nelsen, F. M., and F. T. Eggertsen, 1958, Determination of surface area: Anal. Chem., v. 30, p. 1387-1390.

Purdue University Cooperative Extension Service, 1971, Sources and analyses of liming materials: Report No. 64 (Agronomy Dept.), Lafayette, IN, 25 p.

Segall, T. R., 1972, Michigan mineral producers 1971: Geological Survey Division, Dept. of Nat. Res., Lansing, MI, p. 13.

Thiel, G. A., 1930, A correlation of marl beds with types of glacial deposits: Jour. Geology, v. 38, p. 717-728.

Thomas, Josephus, Jr., and R. R. Frost, 1971, Versatile apparatus for studying reactions involving gas adsorption or evolution: Illinois Acad. Sci. Trans., v. 64, no. 3, p. 248-253.

U. S. Bureau of Mines, 1969, Minerals Yearbook-1968, vols. I-II: Washington, DC, U. S. Govt. Printing Office, p. 1046.

U. S. Bureau of Mines, 1971, Minerals Yearbook-1969, vols. I-II: Washington, DC, U. S. Govt. Printing Office, p. 1038.

Wilson, S. D., 1970, Suggested method of test for moisture-density relations of soils using Harvard compaction apparatus, in ASTM, Special procedures for testing soil and rock for engineering purposes, Spec. Tech. Pub. 479, p. 101-103.

APPENDIX 1

ANNOTATED BIBLIOGRAPHY ON MARLS IN THE NORTHEASTERN QUARTER OF THE UNITED STATES

This bibliography includes works on fresh-water marls that formed in lakes and bogs in the northeastern quarter of the United States. In the United States such marls occur as commercial deposits only within this area. Deposits of so-called marine marls from the Atlantic Coast have been excluded.

CONNECTICUT

Perry, J. B., 1873, Hints toward the post-Tertiary history of New England from personal study of rocks, with strictures on Dana's "Geology of the New Haven region": Boston Soc. Nat. Hist. Proc., v. 15, p. 48-148.

Discussion of the marl and peat periods of post-Pliocene time.

ILLINOIS

Athy, L. F., 1928, Geology and mineral resources of the Herscher Quadrangle: Illinois Geol. Survey Bull. 55, 120 p.

Marl described (p. 108-109).

Baker, F. C., 1912, Postglacial life of Wilmette Bay, glacial Lake Chicago: Illinois Acad. Sci. Trans. (1911), v. 4, p. 108-116.

Describes a marl bed about 5 inches thick (p. 109, 111-112).

Baker, F. C., 1918, Postglacial Mollusca from the marls of Central Illinois: Jour. Geol., v. 26, no. 7, p. 659-671.

Describes 8- to 12-inch thick marl bed on campus of University of Illinois, Urbana (p. 660). Refers to marls from Maine (p. 661-663, 665).

Decker, C. E., 1912, A tufa deposit near Danville, Illinois: Illinois Acad. Sci. Trans., v. 5, p. 109-111.

An unsuccessful search was made for this deposit in July 1971.

Lamar, J. E., 1938, Unexploited or little known industrial minerals of Illinois: Illinois Geol. Survey Circ. 23, p. 213-232.

Describes shell marl localities in Illinois (p. 220-221).

Lamar, J. E., 1965, Industrial minerals and metals of Illinois: Illinois Geol. Survey Ed. Ser. 8, 48 p.

Brief account of deposits of marl, tufa, and travertine in Illinois. Includes names of counties in which some deposits have been worked (p. 46).

Mosier, J. G., S. V. Holt, F. A. Fisher, E. E. DeTurk, H. J. Snider, and L. H. Smith, 1923, Livingston County soils: Univ. of Illinois Agr. Exp. Sta. Soil Rept. 25, 55 p.

Reports muck on marl in SE¼ Sec. 32, T. 30 N., R. 7 E. (p. 27).

Powers, W. E., 1936, Geological setting of the Aurora mastodon remains: Illinois Acad. Sci. Trans. (1935), v. 28, no. 2, p. 193-194.

Reports occurrence of 30 feet of marl (p. 193).

Rubey, W. W., 1952, Geology and mineral resources of the Hardin and Brussels Quadrangles (Illinois): U. S. Geol. Survey Prof. Paper 218, 179 p.

Describes calcareous tufa deposits (p. 97-98).

INDIANA

Blatchley, W. S., and G. H. Ashley, 1901, The lakes of northern Indiana and their associated marl deposits: in W. S. Blatchley, Indiana Dept. Geol. and Nat. Resources, 25th Ann. Rept. (1900), p. 31-321.

McGregor, D. J., 1958, Cement raw materials in Indiana: Indiana Geol. Survey Bull. 15, 88 p.

Use of marls in cement in Indiana (p. 14). Discussion of marl (p. 45, 49); analyses of marls (p. 50).

Wayne, W. J., 1963, Pleistocene formations in Indiana: Indiana Geol. Survey Bull. 25, 85 p.

Martinsville Formation defined to include a paludal facies with calcareous marl (p. 28-31). Refers to sections of Martinsville Formation that contain marl (p. 80).

Wayne, W. J., 1971, Marl resources of Indiana: Indiana Geol. Survey Bull. 42-G, 16 p.

Distribution, production, and analyses of marl deposits in Indiana.

MAINE

Dodge, J. R., 1868, On the limestone and pond-marls of Maine: U. S. Agricultural Rept., p. 370-371.

Description of formations and localities with analyses; special reference to fertilizing qualities.

MASSACHUSETTS

Hitchcock, Edward, 1833, Report on the geology, mineralogy, botany, and zoology of Massachusetts: Amherst: J. S. and C. Adams, xii p., 692 p.

Marl occurrences (p. 38, 120).

Hitchcock, Edward, 1841, Geology of Massachusetts, v. 1: Amherst: J. S. and C. Adams, 299 p.

Discussion of marl with locations (p. 67-75); analyses of marls (p. 70). Discussion of green sand (marl) with analyses (p. 91-95).

MICHIGAN

Cook, C. W., 1912, Michigan cement: Michigan Geol. and Biol. Survey Pub. 8, Geol. Ser. 6, p. 337-354.

Discussion of marls (p. 338-342) and analyses of marls (p. 341). Use of marl by plants (p. 344-350).

Davis, C. A., 1900, A contribution to the natural history of marl: Jour. Geol., v. 8, no. 6, p. 485-497.

Davis, C. A., 1900, A remarkable marl lake: Jour. Geol., v. 8, no. 6, p. 498-503.

Davis, C. A., 1901, A second contribution to the natural history of marl: Jour. Geol., v. 9, no. 6, p. 491-506.

Three papers by Davis describe marl that occurs in certain lakes in Michigan (Montcalm, Branch, and Isabella Counties) and discuss the origin of the marl derived from chemical processes of plants, especially Chara that grows on the bottoms of the lakes.

Hale, D. J., and others, 1903, Marl (bog lime) and its application to the manufacture of portland cement: Michigan Geol. Survey, v. 8, pt. 3, 399 p.

Klyce, D. F., and R. J. Bishop, 1971, Mineral industry of Michigan 1969: Michigan Geol. Survey Ann. Statistical Summ. 13, 18 p.

Agricultural production of marl (p. 8). Quantity and value of marl production for 1968 and 1969 (p. 9). Principal marl producers listed (p. 18).

Segall, R. T., 1972, Michigan mineral producers 1971: Michigan Geol. Survey Ann. Directory 4, 52 p.

List of marl producers (p. 13).

MINNESOTA

Armstrong, L. C., 1927, The geologic conditions favorable for the accumulation of marl, with special reference to east central Minnesota: Univ. of Minnesota, Minneapolis, E. M. thesis.

Emmons, W. H., and F. F. Grout, eds., 1943, Mineral resources of Minnesota: Minnesota Geol. Survey Bull. 30, 149 p.

Section on marls (p. 101-105, 108); includes map of distribution and number of deposits per county.

Kirk, R. E., 1926, The manufacture of portland cement from marl: Univ. of Minnesota Eng. Expt. Sta. Bull. 4.

Roepke, H. H., 1958, The Nisswa Lake marl deposit, Crow Wing County, Minnesota: Univ. of Minnesota, Minneapolis, M.S. thesis.

See G. M. Schwartz below.

Schwartz, G. M., et al., 1959, Investigation of the commercial possibilities of marl in Minnesota: St. Paul: Office of Iron Range Resources and Rehabilitation (in coop. with the Minnesota Geol. Survey and Univ. of Minnesota, Minneapolis), xiii p., 99 p.

Among other subjects related to production and uses of marl, this book contains chapters on methods of chemical analyses of marl, investigation of marl deposits, and experiments on drying marl. Chapter IV is a reprint of H. H. Roepke's thesis on the Nisswa Lake marl deposit.

Appendix A is a reprint of C. R. Stauffer and G. A. Thiel's paper, 1933, "The limestones and marls of Minnesota": Minnesota Geol. Survey Bull. 23, pt. II (p. 79-190).

Minnesota Geological Survey. Marl: Minnesota Geol. Survey Misc. Rept. 8, 3 p.

Defines marl and lists five large marl deposits in Minnesota. Counties having large marl tonnages include Crow Wing, Wright, and Stearn. Lists uses of limestone and marls.

Stauffer, C. R., and G. A. Thiel, 1933, The limestones and marls of Minnesota: Minnesota Geol. Survey Bull. 23, 193 p.

Uses of marl (p. 1-8). Part II, "The marls of Minnesota" (p. 79-190) has been reprinted as Appendix A in G. M. Schwartz et al., 1959.

Thiel, G. A., 1930, A correlation of marl beds with types of glacial deposits: Jour. Geol., v. 38, no. 8, November-December, p. 717-728.

Thiel, G. A., 1946, Marl: Conservation Volunteer, v. 9, no. 51, March-April, p. 13-15.

Zumberge, J. H., 1952, The lakes of Minnesota, their origin and classification: Minnesota Geol. Survey Bull. 35, xiii p., 99 p.

Discussion of marls in lakes (p. 69, 71-72).

NEW HAMPSHIRE

Hitchcock, C. H., 1874, The geology of New Hampshire: Part I. Physical geography: Concord, NH: Edward A. Jenks, xi p., 667 p.

Information on marl localities (p. 549).

Hitchcock, C. H., 1878, The geology of New Hampshire: Part V. Economic geology: Concord, NH: Edward A. Jenks, 103 p.

Gives marl localities (p. 95).

NEW JERSEY

Cook, G. H., 1868, Geology of New Jersey: Newark, xxiv p., 899 p.

Discussion of shell-marl, calcareous sinter, calcareous tufa, and travertine (p. 170-172).

Kummel, H. B., 1901, Report on the portland cement industry: New Jersey Geol. Survey Ann. Rept. of the State Geologist for the year 1900, pt. 2, p. 9-101.

Numerous and very small lake deposits of marl are described (p. 98-101); analyses (p. 98).

NEW YORK

Graham, J. A., 1955, The mineral industries of New York State 1949-1959: New York State Mus. and Science Service Circ. 41, 76 p.

Report of one marl producer in Livingston County in 1949 giving quantity and value of production (p. 30).

Hartnagel, C. A., 1927, The mining and quarry industries of New York from 1919 to 1924 including lists of operators: New York State Mus. Bull. 273, 102 p.

Marl discussed (p. 52-54). Dunkirk operator reporting production in 1924.

Hartnagel, C. A., and J. G. Broughton, 1951, The mining and quarry industries of New York State, 1937 to 1948: New York State Mus. Bull. 343, 130 p.

Use of marl in portland cement (p. 23-24).

Luedke, E. M., C. T. Wrucke, and J. A. Graham, 1959, Mineral occurrences of New York State with selected references to each locality: U. S. Geol. Survey Bull. 1072-F, p. iii, p. 385-444.

Marl occurrences (p. 420-421).

Newland, D. H., 1912, The mining and quarry industry of New York State: Report of operations and production during 1911: New York State Mus. Bull. 161, 114 p.

Marl discussed (p. 80-81).

Newland, D. H., 1921, The mineral resources of the state of New York: New York State Mus. Bull. 223, 224 (1919), 315 p.

Marl discussed (p. 145-149); chemical analyses (p. 147).

Newland, D. H., and C. A. Hartnagel, 1936, The mining and quarry industries of New York State for 1930 to 1933: New York State Mus. Bull. 305, 95 p.

Discussion of marl (p. 48-52). Little marl now being produced (p. 51-52).

Ries, Heinrich, and E. C. Eckel, 1901, Lime and cement industries of New York: New York State Mus. Bull., v. 8, no. 44, 968 p.

OHIO

Kefauver, Hazel, ed., 1960, Annual coal and nonmetallic mineral report with directories of reporting firms for 1960: Ohio Dept. Indus. Relations, 290 p.

One marl producer listed (p. 244).

Stout, Wilber, 1940, Marl, tufa rock, travertine, and bog ore in Ohio: Ohio Geol. Survey Bull. 41, 56 p.

PENNSYLVANIA

Dickey, J. B. R., 1923, Calcareous marl in Pennsylvania south of the terminal moraine: Pennsylvania Geol. Survey Bull. 76, 10 p.

Miller, B. L., 1934, Limestones of Pennsylvania: Pennsylvania Geol. Survey Bull. M 20, 729 p.

Marl deposit in Crawford County described (p. 332-335); analyses (p. 335). General discussion of marls (p. 54-56). Repeats descriptions of marls from Dickey (1923) (p. 167, 292, 345-346, 388, 394, 423, 499, and 700). Describes concretions (p. 475-477). Reports marl locations (p. 387 and 714).

VERMONT

Hitchcock, Edward, Edward Hitchcock, Jr., A. D. Hager, and C. M. Hitchcock, 1861, Report on the geology of Vermont: descriptive, theoretical, economical, and scenographical, Vols. I and II: Claremont Manufacturing Company, Claremont, NH, 988 p.

Marls discussed (p. 167-171, 725-726, and 805-806); analyses (p. 168, 697-698, and 805).

VIRGINIA

LeVan, D. C., 1971, Directory of the mineral industry in Virginia—1971: Virginia Div. of Mineral Resources, 46 p.

Lists four marl producers (p. 27-28), one fresh-water marl producer (J. C. Digges), and three producers of marine shell marls.

McGill, W. M., 1936, Outline of the mineral resources of Virginia: Virginia Geol. Survey Bull. 47, Ed. Ser. No. 3, 81 p.

Calcareous (shell) marl and travertine discussed (p. 36).

WEST VIRGINIA

Davies, W. E., 1949, Caverns of West Virginia: West Virginia Geol. Survey, v. 19, x p., 353 p.

Marl deposits (p. 5). Shelter caves present in marl bed at Williamsport (p. 60).

Gillespie, W. H., and J. A. Clendening, 1964, An interesting marl deposit in Hardy County, West Virginia: West Virginia Acad. Sci. Proc., v. 36, p. 147-151.

Grimsley, G. P., 1906, Clays, limestones, and cements: West Virginia Geol. Survey, v. 3 (1905), xviii p., 565 p.

Marl reported with analysis (p. 515-516).

Grimsley, G. P., 1916, Jefferson, Berkeley, and Morgan Counties: West Virginia Geol. Survey County Repts., xxvi p., 644 p.

Marl deposits discussed (p. 393-396); analyses (p. 394-396).

McCue, J. B., J. B. Lucke, and H. P. Woodward, 1939, Limestones of West Virginia: West Virginia Geol. Survey, v. 12, xiv p., 560 p.

Marl locations mentioned (p. 98, 102, 115, 153, 204, 211-213, 455, 483-484); analyses of marls (p. 111, 160, 216, 396, 428).

Price, P. H., R. C. Tucker, and O. L. Haught, 1938, Geology and natural resources of West Virginia: West Virginia Geol. Survey, v. 10, xi p., 462 p.

Calcareous tufa, travertine, and calcareous marl described as minor cement materials. Refers to use by only two plants at Charles Town (p. 302, 305).

Reger, D. B., and R. C. Tucker, 1924, Mineral and Grant Counties: West Virginia Geol. Survey County Repts., xxiv p., 866 p.

Discusses marl deposits (p. 675-676); analyses (p. 678); and locations (p. 680).

Tilton, J. L., W. F. Prouty, and P. H. Price, 1927, Pendleton County: West Virginia Geol. Survey County Repts., xviii p., 384 p.

Marls discussed with one location given (p. 289); photograph of outcrop (p. 288).

Tilton, J. L., W. F. Prouty, R. C. Tucker, and P. H. Price, 1927, Hampshire and and Hardy Counties: West Virginia Geol. Survey County Repts., xxii p., 624 p.

Travertine locations given (p. 18 and 138). Photograph of marl deposit (p. 140). Marl analyses (p. 274, 308, 554). Marl deposits discussed (p. 274, 308).

Woodward, H. P., 1951, Ordovician System of West Virginia: West Virginia Geol. Survey, v. 21, xi p., 627 p.

Discusses marl deposits in vicinity of Charles Town (p. 487).

WISCONSIN

Natural Resources Committee of State Agencies of Wisconsin, 1956, The natural resources of Wisconsin: Wisconsin Nat. Resources Comm. of State Agencies, 159 p.

Marl discussed (p. 109). Gives production of agricultural lime of four counties in 1952.

Ostrom, M. E., 1970, Directory of Wisconsin mineral producers. 1968: Wisconsin Geol. and Nat. History Survey Inf. Circ. 12, 68 p.

One marl producer listed (p. 57).

Steidtmann, Edward, 1924, Limestones and marls of Wisconsin: Wisconsin Geol. and Nat. History Survey Bull. 66, 208 p.

Origin of marls (p. 6); the marls of Wisconsin (p. 128-153); uses of marl (p. 98, 111-116).

APPENDIX 2

SOURCES OF SAMPLES AND REMARKS ON THE DEPOSITS

Number	Thickness represented (ft)	Type	Source, location, and quadrangle map	Remarks on the deposit and geologic unit sampled
7120	35	Chalky coquina	Houdaille-Duval-Wright Co. quarry, 5 mi NE of Newberry, FL; SE¼ Sec. 23, 9S-17E (Newberry Quad., FL).	Extensive deposit in the Crystal River Formation (Eocene).
7121A 7121B	0.5 3.5+	Shells and broken shells	Turtle Beach of Siesta Key, offshore bar, 3 mi N and 2 mi W of Osprey, FL; SE¼ Sec. 23, 37S-18E (Bird Keys Quad., FL).	No notable deposit at this locality. Samples considered typical of coquina limestone and shells of the Anastasia Formation (Pleistocene), which occurs for many miles south of Turtle Beach along the Gulf Coast.
7122A 7122B	2 5	Coquina	J. Cochran pit, 4 mi W and 2 mi N (off Rt. 80) of La Belle, FL; SE¼ Sec. 13, 43S-28E (Sears Quad., FL).	Operating pit extends over about 5 acres in the Caloosahatchee Marl (Pleistocene).
7123	4	Calcareous sandy marl	Outcrop on north bank of Caloosahatchee River, north side of La Belle, FL; SE¼ Sec. 32, 42S-29E (La Belle Quad., FL).	Sandy facies of Caloosahatchee Marl (Pleistocene).
7124	10+	Clam shells	Radcliff Materials, Inc., Mobile, AL. Lake Pontchartrain, LA (30°10'N, 90°05'W).	Dredging operation in Lake Pontchartrain, LA (Holocene).
7125	10+	Oyster shells	Radcliff Materials, Inc., Mobile, AL. Mobile Bay, AL (30°32'N, 88°02'W).	Dredging operation in a dead oyster reef in Mobile Bay, AL (Holocene).
7126A 7126B	15 2.5	Bog marl	Woodrow Gary, New Madison, OH. Pit location in SE¼ SW¼ Sec. 1, 10N-1E (New Madison Quad., OH).	Former operations extended over about a 5-acre bog (Pleistocene). Upper beds exposed near center of deposit.

7127A	0.5	Tufaceous bog marl	Abandoned pit, 1.3 mi N of intersection Rt. 269 and NYC RR at Castalia, OH, and 0.65 mi W. In Resthaven Wildlife Area (Castalia Quad., OH).	Sample from plowed surface of a 10-acre field adjacent to an extensive bog deposit formerly operated by a cement company (Pleistocene).
7127B	0.8	Clayey and marly silt		0.5 to 0.8 ft below sample 7127A above.
7127C	2.5	Clayey and marly silt		0.8 to 3.8 ft below sample 7127A above.
7127D		Tufaceous bog marl		Typical of the large bumps present in deposit (Pleistocene).
7128A	1.0	Tufaceous bog marl	Abandoned pit in road embankment. 0.6 mi S of 7127 (Castalia Quad., OH).	Same deposit as 7127 0.5 ft to 1.5 ft below surface of embankment.
7128B	1.5			Same deposit as 7127 1.5 ft to 3.0 ft below surface of embankment (Pleistocene).
7129	15	Tufaceous bog marl	Abandoned pit, SE¼ SE¼ Sec. 15, 20N-15W, 1.1 mi SW of McZena, OH (Loudonville Quad., OH).	Sample from edge of old road bed used during production of marl from a moderate size bog. Probably typical of marl underlying the small lake 20 yards to the west (Pleistocene).
7130	2.5	Bog marl	Abandoned pit, 0.7 mi S of intersection Rt. 424 and Frisbee Rd. and 0.2 mi due east (Cassadaga Quad., NY).	Old portland cement plant. Sample from below 1.5 ft of muck and adjacent to water-filled pit in a moderately extensive bog (Pleistocene).
7131A	1.9	Bog marl	Jasper Robinson, 0.5 mi SW of Clarendon, NY (Holley Quad., NY).	Samples from a 10 to 15 acre area (Pleistocene)
7131B	3.5			
7131C	1.5			
7132A	2.8	Bog marl	Scofield Lime Products, Fancher, NY 14452. Pit 0.5 mi S of intersection of Rt. 19 and New York Throughway and 0.1 mi W of Rt. 19 (Churchville Quad., NY).	Commercial operation in a Pleistocene bog. Sample A from upper marl, center of pit.
7132B	5.5+			Sample of marl under 7132A.
7132C	6			Sample of the upper part of the marl in the north end of the pit.
7132D	20			Sample from stockpile.

APPENDIX 2, continued

Number	Thickness represented (ft)	Type	Source, location, and quadrangle map	Remarks on the deposit and geologic unit sampled
7133	5.5	Tufaceous bog marl	Abandoned pit of the Genesee Lime Products Co., Rochester, NY. Pit located 1.0 mi E and 0.8 mi N of Caledonia, NY (Caledonia Quad., NY).	Sample from auger hole in an extensive bog (Pleistocene).
7134A	1.5	Lake marl	Abandoned pit 0.9 mi SW (on Rt. 245) of Wayland, NY (Wayland Quad., NY).	Extensive areal deposit (Pleistocene). Sample from auger hole on edge of lake. Marl is underlain by muck and gravel at the site of the auger hole.
7135	1.0	Clayey and peaty marl	John Underwood, Camillus, NY. Pit located 1 mi S and 1 mi W of Warners, NY (Camillus Quad., NY).	Abandoned portland cement pit and plant. Workings in an extensive (Pleistocene) bog.
7136	2.0	Tufaceous bog marl	Outcrop under Penn. Cent. Railroad bridge over Letort Spring Run Creek in Carlisle, PA (Carlisle Quad., PA).	Very limited deposit (Pleistocene).
7137	20	Bog marl	J. C. Digges & Sons, White Post, VA. Pit and plant located $\frac{1}{4}$ mi S of Rt. 617 at point 0.65 mi E of intersection of Rts. 255 and 617, near Briggs (Boyce Quad., VA).	Commercial operations in an extensive bog deposit (Pleistocene) above water table. Sample representative of pit production.
7138	5.5	Lake marl	Sampsel & Son, R.R. 1, Rochester, IN. Pit on east side of Lake 16, 2 mi E of Athens, IN, NW$\frac{1}{4}$ SE$\frac{1}{4}$ Sec. 16, 30N-4E, Fulton Co. (Akron Quad., IN).	Discontinued operations. Sample from above water level. More than 4 ft of similar marl occurs below the beds sampled (Pleistocene).

7139	10-12	Bog marl	Stanley Custer, R.R. 1, Box 1, Milford, IN. Pit on east side of Rt. 15 on the north edge of Milford, IN, NW¼ NE¼ Sec. 8, 34N-6E, Kosciusko Co. (Milford Quad., IN).	Discontinued operation. Sample from stockpile from a 4 to 6 acre bog (Pleistocene).
7140	5.5+	Lake marl	Raymond Beezley, R.R. 4, Albion, IN. Erdly pit located on Whirledge Lake 1 3/4 mi E of Kimmell, IN, Cen. E½ NE¼ Sec. 19, 34N-9E, Noble Co. (Ligonier Quad., IN).	Commercial operations on the east side of lake. Sample from stockpile of Pleistocene marl.
7141	7+	Bog marl	Vernon Kaufman, R.R. 1, Topeka, IN. Fought pit located 3 mi E and 1 mi S of Topeka, IN, NW¼ NW¼ NW¼ Sec. 3, 35N-9E, Noble Co. (Oliver Lake Quad., IN).	Commercial operations in a Pleistocene bog. Sample from stockpile.
7142	16-18	Lake marl	Miller Marl Co., R.R. 1, Middlebury, IN. Pit on south end of Cass Lake, 3 mi E of Middlebury, NW¼ Sec. 5, 37N-8E, La Grange Co. (Middlebury Quad., IN).	Commercial operations. Sample from stockpile of Pleistocene marl.
7143A	?	Bog marl	K. Fleming, Fremont, IN. Pit on west edge of Fremont, SW¼, SE¼ Sec. 20, 38N-14E, Steuben Co. (Angola East Quad., IN).	Abandoned pit in a large Pleistocene bog. Sample from stockpile.
7144A	12-18	Lake marl	Taylor & Son, R.R. 2, Fremont, IN. Garman Pit on Warner Lake, 1½ mi E and 1 mi S of Orland, Cen. W½ Sec. 27, 38N-12E, Steuben Co. (Orland Quad., IN).	Commercial operations in a Pleistocene lake. Sample from stockpile.

APPENDIX 2, continued

Number	Thickness represented (ft)	Type	Source, location, and quadrangle map	Remarks on the deposit and geologic unit sampled
7145A	?	Lake marl	Harlan Spoor, R.R. 1, Burlington, MI. Pit is 0.2 mi S of R Drive S Rd., 2.5 mi NW of Burlington, Cen. N½ Sec. 21, 4S-7W, Calhoun Co. (Union City Quad., MI).	Commercial operation in a Pleistocene lake. Sample from stockpile.
7146A	10-15	Lake marl	Darrell Hamilton, Nashville, MI. Pit on south side of Thornapple Lake, 4 mi W of Nashville, NE¼ NW¼ NE¼ Sec. 30, 3N-7W, Barry Co. (Nashville Quad., MI).	Commercial operation on the southeast edge of a Pleistocene lake. Sample from stockpile.
7147A	20+	Bog marl	S. K. Vorres, Fremont, MI. Pit is 5 mi N of Fremont, on the east side of Luce Rd., Cen. Sec. 6, 13N-13W, Newaygo Co. (White Cloud Quad., MI).	Location of pit from which marl (Pleistocene) was dug for full-scale tests by TVA. Sample from depleted stockpile.
7148	4+	Tufaceous marl (spring deposit)	Grant Tufa Lime Co., Grant, MI. Pit is 7 mi E of Grant, NW¼ NE¼ Sec. 29, 11N-11W, Newaygo Co. (Sand Lake Quad., MI).	Abandoned operations in a Pleistocene spring deposit.
7149A	1-4	Tufaceous bog marl	Gerald Arnsman, R.R. 1, Hopkins, MI. Belden Pit, 0.5 mi E of South Monterey, MI, SE¼ SE¼ NW¼ Sec. 34, 3N-13W, Allegan Co. (Allegan Quad., MI).	Commercial operation in a Pleistocene bog. Sample A from upper tufaceous beds in center of pit.
7149B	12+	Bog marl		Sample B from lower beds.

7150	20	Lake marl	Leon Hayward Dry Marl, R.R. 2, Vicksburg, MI. Marl is dredged from beneath the south side of Indian Lake, 3 mi NE of Vicksburg in Sec. 8, 4S-10W, Kalamazoo Co. (Leonidas Quad., MI).	Commercial operations in Pleistocene lake. Sample from stockpile.
7151A 7151B 7151C	20+	Bog marl	Poehlman & Sons, R.R. 2, Cassopolis, MI. Operations are 6 mi SW of Cassopolis, SE¼ NE¼ Sec. 13, 7S-16W, Cass Co. (Cassopolis Quad., MI).	Commercial operations in Pleistocene marl. Samples of three typical marl types from the pit.
7152	5+	Bog marl	Lime Products Co. Former dredging 3.5 mi N of Eagle, WI, in SW¼ SE¼ Sec. 34, 6N-17E, Waukesha Co. (Eagle Quad., WI).	Abandoned operation in a Pleistocene bog. Samples represent upper 4 ft of marl at three different places along former workings. Area is within Kettle Moraine State Forest.
7153	—	Sludge from paper mfg. plant	Nekoosa Edwards Paper Co., Port Edwards, WI. Sludge pond east side of river at Nekoosa, WI, SE¼ Sec. 10, 21N-5E, Wood Co. (Wisconsin Rapids Quad., WI).	Waste product from Kraft paper process, sold to area farmers as ag lime, consists of more than 95% $CaCO_3$.
7154	5-10	Bog marl	Floyd Helgeson, R.R. 1, Iola, WI. Pit 3 mi NW of Iola, SW¼ NE¼ Sec. 21, 24N-11E, Waupaca Co. (Tigerton Quad., WI).	Dredging operations have been discontinued in a Pleistocene bog. Sample from stockpile.
7155	3.5+	Lake marl	Clifford Caldwell Marl Co., Scandinavia, WI. Pit is on south side of Marl Lake, 3 mi SW of Scandinavia, W½ NW¼ Sec. 33, 23N-11E, Waupaca Co. (Waupaca Quad., WI).	Dredging operations have been discontinued in the Pleistocene lake. Sample from the upper 3.5 ft at water's edge.
7156	3.5+	Bog marl	A. E. Stelter, Bloomer, WI. Neitzel pit along O'Neal Creek, 5.5 mi E of Bloomer on Rt. 64, SW¼ SW¼ Sec. 33, 3N-8W, Chippewa Co. (Bloomer Quad., WI).	Abandoned pit in a Pleistocene bog. Sample from upper 3 to 5 ft adjacent to pond.

APPENDIX 2, continued

Number	Thickness represented (ft)	Type	Source, location, and quadrangle map	Remarks on the deposit and geologic unit sampled
7157A	15-18	Lake marl	Burnett County Highway Dept., Siren, WI. Pit located on northeast shore of Wood Lake, 8 mi W and 2 mi S of Siren, NW¼ SE¼ Sec. 27, 38N-18W, Burnett Co. (Milltown Quad., WI).	Operations in a Pleistocene lake deposit. Sample A from stockpile.
7157B	2.5			Uppermost beds of marl.
7157C	3.5			2.5 to 6 ft below top of marl.
7157D	2.0			6 to 8 ft below top of marl.
7158	?	Lake marl	Sorum's Marl Service, Remer, MN. On the south shore of Birch Lake, 2 mi SE of Remer, near Cen. N½ Sec. 8, 141N-25W, Cass Co., MN (Hibbing 1:250,000 Quad., MN).	Commercial operations in a Pleistocene lake deposit. Sample from stockpile.
7159	13	Bog marl	Richard Nanik Marl, Staples, MN. Pit located along Tower Creek, 10.5 mi N of Staples, NE¼ NW¼ Sec. 13, 136N-33W, Wadena Co. (Brainerd 1:250,000 Quad., MN).	Commercial operations in a Pleistocene bog. Sample from upper beds below muck.
7160	2.5	Bog marl	Lily pond on Urbana campus, Univ. of Illinois, near Cen. Sec. 18, 19N-9E, Champaign Co. (Urbana Quad., IL).	Excavation exposure. Sampled in 1947 as NF446 (Pleistocene).
7161	1.0+	Bog marl	Along Blackberry Creek, 5 mi due west of Fox River at Aurora, IL, NE¼ NE¼ SW¼ Sec. 14, 38N-7E, Kane Co. (Geneva Quad., IL).	Outcrop of marl. Sampled in 1933 as NF153 (Pleistocene).

7162A 7162B 7162C 7162D	12+	Bog marl	Delmer Ford, Chatsworth, IL. Located 5 mi S and 2 mi W of Chatsworth along creek north side of road SE¼ SW¼ Sec. 32, 26N-8E, Livingston Co. (Sibley Quad., IL).	Discontinued operations in a Pleistocene bog. Sample from four types of marl from stockpiles.
7163A	4.2+	Bog marl	Batavia Soil Builders. Located 2.5 mi W of Batavia, IL, SW¼ SW¼ Sec. 19, 39N-8E, Kane Co. (Geneva Quad., IL).	Marl occurs under 3 ft of peat. Currently the peat is being produced. Boring taken on the west side of bog. Sample A from lower marl beds (Pleistocene).
7163B	0.2			Sample from middle marl bed.
7163C	5.8			Sample from upper marl beds.
7163D	24			Sample from stockpile near center of north end of bog.

ENVIRONMENTAL GEOLOGY NOTES SERIES

(Exclusive of Lake Michigan Bottom Studies)

* 1. Controlled Drilling Program in Northeastern Illinois. 1965.
* 2. Data from Controlled Drilling Program in Du Page County, Illinois. 1965.
* 3. Activities in Environmental Geology in Northeastern Illinois. 1965.
* 4. Geological and Geophysical Investigations for a Ground-Water Supply at Macomb, Illinois. 1965.
* 5. Problems in Providing Minerals for an Expanding Population. 1965.
* 6. Data from Controlled Drilling Program in Kane, Kendall, and De Kalb Counties, Illinois. 1965.
* 7. Data from Controlled Drilling Program in McHenry County, Illinois. 1965.
* 8. An Application of Geologic Information to Land Use in the Chicago Metropolitan Region. 1966.
* 9. Data from Controlled Drilling Program in Lake County and the Northern Part of Cook County, Illinois. 1966.
*10. Data from Controlled Drilling Program in Will and Southern Cook Counties, Illinois. 1966.
*11. Ground-Water Supplies Along the Interstate Highway System in Illinois. 1966.
12. Effects of a Soap, a Detergent, and a Water Softener on the Plasticity of Earth Materials. 1966.
*13. Geologic Factors in Dam and Reservoir Planning. 1966.
*14. Geologic Studies as an Aid to Ground-Water Management. 1967.
*15. Hydrogeology at Shelbyville, Illinois—A Basis for Water Resources Planning. 1967.
*16. Urban Expansion—An Opportunity and a Challenge to Industrial Mineral Producers. 1967.
*17. Selection of Refuse Disposal Sites in Northeastern Illinois. 1967.
*18. Geological Information for Managing the Environment. 1967.
*19. Geology and Engineering Characteristics of Some Surface Materials in McHenry County, Illinois. 1968.
*20. Disposal of Wastes: Scientific and Administrative Considerations. 1968.
*21. Mineralogy and Petrography of Carbonate Rocks Related to Control of Sulfur Dioxide in Flue Gases—A Preliminary Report. 1968.
*22. Geologic Factors in Community Development at Naperville, Illinois. 1968.
23. Effects of Waste Effluents on the Plasticity of Earth Materials. 1968.
24. Notes on the Earthquake of November 9, 1968, in Southern Illinois. 1968.
*25. Preliminary Geological Evaluation of Dam and Reservoir Sites in McHenry County, Illinois. 1969.
26. Hydrogeologic Data from Four Landfills in Northeastern Illinois. 1969.
27. Evaluating Sanitary Landfill Sites in Illinois. 1969.
*28. Radiocarbon Dating at the Illinois State Geological Survey. 1969.
*29. Coordinated Mapping of Geology and Soils for Land-Use Planning. 1969.
*31. Geologic Investigation of the Site for an Environmental Pollution Study. 1970.
33. Geology for Planning in De Kalb County, Illinois. 1970.
34. Sulfur Reduction of Illinois Coals—Washability Tests. 1970.
*36. Geology for Planning at Crescent City, Illinois. 1970.
*38. Petrographic and Mineralogical Characteristics of Carbonate Rocks Related to Sorption of Sulfur Oxides in Flue Gases. 1970.
40. Power and the Environment—A Potential Crisis in Energy Supply. 1970.
42. A Geologist Views the Environment. 1971.
43. Mercury Content of Illinois Coals. 1971.
45. Summary of Findings on Solid Waste Disposal Sites in Northeastern Illinois. 1971.
46. Land-Use Problems in Illinois. 1971.
48. Landslides Along the Illinois River Valley South and West of La Salle and Peru, Illinois. 1971.
49. Environmental Quality Control and Minerals. 1971.
50. Petrographic Properties of Carbonate Rocks Related to Their Sorption of Sulfur Dioxide. 1971.
51. Hydrogeologic Considerations in the Siting and Design of Landfills. 1972.
52. Preliminary Geologic Investigations of Rock Tunnel Sites for Flood and Pollution Control in the Greater Chicago Area. 1972.
53. Data from Controlled Drilling Program in Du Page, Kane, and Kendall Counties, Illinois. 1972.

---

*Out of print.